

Unsteady Peristaltic Flow with the Interaction of Nanoparticles having Variable Viscosity



**Name: Sidra Yousaf
Reg. # 00000103732**

**This thesis is submitted as a partial fulfillment of the requirements for
the degree of
Master of Science in
Mathematics**

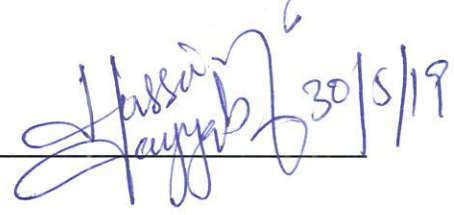

**Supervised by: Dr. Noreen Sher Akbar
Department of Mathematics
School of Natural Sciences (SNS)**

**National University of Sciences and Technology (NUST)
H-12, Islamabad, Pakistan**

2019.

National University of Sciences & Technology**MS THESIS WORK**


We hereby recommend that the dissertation prepared under our supervision by: Sidra Yousaf, Regn No. 00000103732 Titled: **Unsteady Peristaltic Flow with the Interaction of Nanoparticles having Variable Viscosity.** accepted in partial fulfillment of the requirements for the award of **MS** degree.

Examination Committee Members1. Name: DR. MERAJ MUSTAFA HASHMISignature: 2. Name: DR. SYED TAYYAB HUSSAIN SHAHSignature:  30/5/19External Examiner: DR. RAHMAT ELLAHISignature: Supervisor's Name DR. NOREEN SHER AKBARSignature: 


Head of Department

30/5/2019
Date

COUNTERSIGNEDDate: 30/5/19


Dean/Principal


THESIS ACCEPTANCE CERTIFICATE

Certified that final copy of MS thesis written by Ms. Sidra Yousaf (Registration No. 00000103732), of School of Natural Sciences has been vetted by undersigned, found complete in all respects as per NUST statutes/regulations, is free of plagiarism, errors, and mistakes and is accepted as partial fulfillment for award of MS/M.Phil degree. It is further certified that necessary amendments as pointed out by GEC members and external examiner of the scholar have also been incorporated in the said thesis.

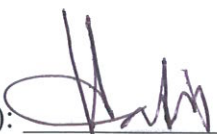
Signature: 

Name of Supervisor: Dr. Noreen Sher Akbar

Date: 30/5/19

Signature (HoD): 

Date: 30/5/2019

Signature (Dean/Principal): 

Date: 30/5/19

**In the name of ALLAH, the Gracious, the
Merciful**

Dedicated to

**My beloved parents Muhammad Yousaf,
Irshad Bibi and my siblings Muhammad
Mohsin, and Abu-Bakkar.**

Acknowledgements

First of all, I would like to thank **Allah Almighty**, who has given me the aptitude, nerve and His blessings to complete this thesis. He gave me power and right path throughout my research work.

My special and earnest thanks to my kind supervisor, **Dr. Noreen Sher Akbar** for providing me the most pacific environment to work and guiding me throughout my research work. A special thanks to my guidance and evaluation committee members, **Dr. Meraj Mustafa** and **Dr. Syed Tayyab Hussain Shah**, for their valuable guidance, suggestions and encouragement. I am grateful especially to **School of Natural Sciences, NUST** for providing me all the amenities and a platform to work. I greatly acknowledge the facilities and technical support provided by other schools of NUST.

Finally, I would like to convey my gratitude to all friends for their help, guidance and prayers. I would like to thank my family especially my father **Muhammad Yousaf**, my mother **Irshad Bibi**, my brothers **Muhammad Mohsin**, **Abu-Bakkar** and my friend **Ayesha Ayub** for being so supportive and for their love.

Sidra Yousaf

Abstract

An analytical analysis of Carbon nanotubes(CNTs) with variable viscosity is done to scrutinize the unsteady peristaltic flow in a non-uniform pipe of finite measure. Exact solutions are obtained. Influence of CNTs on temperature, axial and transverse velocities, effective thermal conductivity and on pressure gradient is studied graphically by varying various flow constraints. Trapping has also been examined. This study is helpful in medication and even essential to layout a micro push for the movement of nanofluids.

Contents

1. Introduction -----	1
2. Carbon Nanotube Analysis for an Unsteady Physiological Flow in a Non-Uniform Channel of Finite Length -----	4
2.1. Introduction -----	4
2.2. Mathematical formulation -----	4
2.3. Analytical solution -----	8
2.4. Graphical representations and discussion -----	9
2.5. Conclusions -----	17
3. Pressure Driven Peristaltic Flow Study with the Interaction of Nanoparticle -----	18
3.1. Introduction -----	18
3.2. Mathematical formulation -----	18
3.3. Analytical solution -----	21
3.4. Graphical representations and discussion -----	23
3.5. Conclusions -----	37

Chapter 1

Introduction

Peristalsis is the process of contraction and relaxation of muscles in a wave like manner. For example, in esophagus where food bolus is swallowed and moved through different processing units of digestive tract. Peristalsis is an automatic process. This process also occurs in Peristaltic pumps where different variety of fluids¹ are displaced. The similar mechanism is used by earthworms to drive their locomotion. In 1987, Pozrikidis C [1] studied the two-dimensional² peristaltic flow by considering creeping motion under which the problem is framed via boundary integral method for Stokes flow. The results are conferred with allusion to different engineering and physiological processes. It is recommended that peristaltic flow by taking different mean pressure gradient under the quasi-steady estimation provides a competent method for molecular-convective transport. In 1982, Radhakrishnamacharya G [2] analyzed the two-dimensional peristaltic motion of a power law fluid by considering long wavelength in contrast to the half-width of the channel. The mathematical expressions for shear stress, stream function and axial pressure gradient are derived and the influence of flow behaviour index n on shear stress and streamline design is studied. Trapping is also discussed. Li M [4] discussed fluid flow and heat transfer attributes of nanofluids in free and forced convection flows by taking suspended solid nanoparticles in base fluids and concluded that suspended nanoparticles³ distinctly changed the heat transfer characteristics and transport properties of suspension. Bhatti MM [6] explored the peristaltic blood flow of nanofluid⁴ in a porous irregular channel with long wavelength estimation and creeping flow scheme. By using perturbation method, the approximated analytical solutions are acquired for pressure rise, friction force, nanoparticle concentration and temperature profiles. To obtain the expression for friction forces and

¹ A fluid is a substance that continuously deforms under a shear stress applied on it.

² The flow in which the variation of flow characteristics can be defined by two spatial coordinates.

³ Particles that lie between 1 to 100 nanometer in size.

⁴ The fluids that contain nanoscale particles.

pressure rise the Numerical computation is used. The influence of distinct physical constraints such as thermal grashof number⁵, thermophoresis parameter, Brownian motion parameter and basic density grashof number on concentration profile, temperature and velocity and profile are discussed with the help of graphs. This analysis has applications in various drug delivery systems in peristaltic pumping and pharmacological engineering.

Contemporary developments in fluid mechanics integrated the areas of the nanofluids and peristaltic motion. Nanoparticles are particles in nanofluids which have extensive span of implementations in biomedical sciences, engineering and in industrial sectors. Bhatti MM [7] examined the peristaltic motion of fluid containing suspended particles through an irregular annulus to examine the heat transfer analysis on clot blood model. Akbar NS [10] analytically analyzed the curved channel with peristaltic transport of copper nanofluids having compliant walls, by considering low Reynolds number⁶ and long wavelength estimation. The mathematical analysis is done and exact solutions for temperature and velocity profile are acquired and the influence of consequential constraints are expressed graphically.

Carbon nanotubes have cylindrical structure and are allotropes of carbon. SWCNT and MWCNT are main types of carbon nanotubes. Akbar and Butt [13] considered curved channel and observed the consequences of heat transfer on peristaltic flow of carbon nanoparticles. By considering low Reynolds number estimation and long wavelength assumption and also by investigating the impacts of curvature of the curved channel, the equations for flow and heat transfer are obtained. Fluid velocity in the curved channel is determined from the exact solution for stream function. The consequence of heat transfer in this channel is perceived and the consequences of Grashof number and curvature parameter on velocity and the pressure gradient are also examined. In 2016, Bhatti et al [18] analyzed the consequences of variable magnetic field of jaffery fluid on peristaltic flow in an irregular rectangular duct with compliant walls by considering the unsteady incompressible viscous electrically conducting flow. Kuznetsov AV & Nield DA [24] examined analytically the natural convective boundary-layer flow of a

⁵ The ratio of buoyancy to viscous forces. Generally it is denoted as Gr. It is a dimensionless quantity.

⁶ The ratio of inertial to viscous forces. It is a dimensionless quantity. It determines whether the fluid is steady or unsteady, streamlined, laminar or turbulent.

nanofluid through a vertical plate and the model used by them is consolidated the consequences of thermophoresis and Brownian motion. Tripathi D [29] proposed a mathematical model based on viscoelastic fluid flow. Low Reynolds number estimation and long wavelength assumption is used to obtain the simplified version of governing equations. With the help of homotopy analysis method the analytical approximate solutions are obtained. Tripathi D [33] presented the numerical study to analyze the peristaltic transport of fractional bio-fluids through the channel by taking assumptions of low Reynolds number and long wavelength. Buongiorno J [36] done numerical analysis over an exponential stretching sheet to examine the boundary layer flow behavior and heat transfer attributes of a nanofluid. Huda AB [40] analyzed the flow of nanofluid and heat transfer in a vertical tube with variable viscosity. A Tiwari-Das type construction is engaged for the nanofluid with a viscosity amendment. Tripathi D [41] investigated the peristaltic flow of nanofluids based on low Reynolds number and the long wavelength approximations through a two-dimensional channel. NS Akbar [42] presented the CNT analysis for an unsteady flow⁷ in two dimensional irregular channel of finite measure. CNTs influence on active thermal conductivity, pressure gradient, axial and transverse velocities, and on temperature are studied graphically by varying various flow constraints. Trapping is also discussed. Our work is done by considering variable viscosity in the unsteady peristaltic flow in a non-uniform channel of finite measure. This study is helpful in medication and even essential to layout a micro push for the movement of nanofluids.

⁷ The flow in which fluid properties change with time is known as unsteady flow.

Chapter 2

Carbon Nanotube Analysis for an Unsteady Physiological Flow in a Non-Uniform Channel of Finite Length

2.1. Introduction:

In this chapter a Carbon nanotubes(CNTs) analysis is done to examine the unsteady peristaltic flow in an irregular channel of certain measure. Exact solutions are obtained. Influence of CNTs on temperature, axial and transverse velocities, effective thermal conductivity and on pressure gradient is studied graphically . Trapping is also examined.

2.2. Mathematical formulation:

In this chapter we have considered the unsteady peristaltic flow of nanofluid with SWCNT and MWCNT via a non-uniform channel of finite measure. The geometrical model is taken as:

$$\tilde{h}(\tilde{\zeta}, \tilde{t}) = a'(\tilde{\zeta}) + b \cos \frac{\pi}{\lambda} (\tilde{\zeta} - c\tilde{t}). \quad (2.1)$$

In above equation; $a'(\tilde{\zeta}) = a_0 + \alpha \tilde{\zeta}$ denotes the half width of the channel at any axial distance $\tilde{\zeta}$ from inlet, $\tilde{\zeta}$ represents the axial coordinate, a_0 gives the half width of channel at inlet, λ is wavelength, b denotes amplitude, c represents wave speed, \tilde{t} is time and α is non-uniformity constant, as $\alpha \rightarrow 0$, the irregular channel moderates to a regular channel.

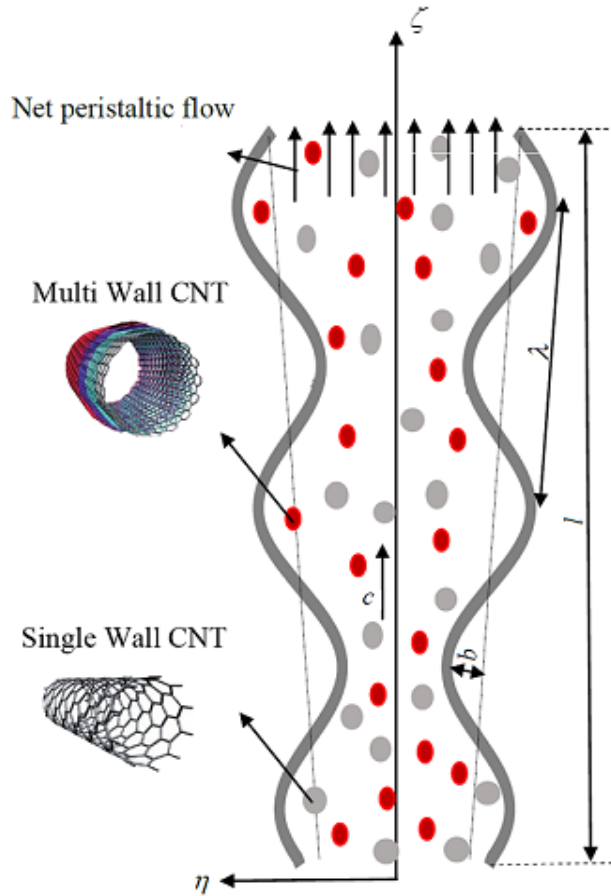


Fig. 2.1: Schematic of the problem.

Consider an irregular channel of finite measure with sinusoidal motion along with the flow path. The walls of this irregular channel are assumed to be alike in structure and distensible. The features of damping are discounted. Governing equations are amended with low Reynolds number and also long wavelength approximation is taken into account. T_1 denotes the extent of the temperature at the wall ($\eta = h$). According to Boussinesq interpretation, the transport equations with a particular reference pressure are described in Ref: [35] for the scheme and subsequent assumptions are considered as: (a) Streamline flow with constant density, (b) negligible external forces, (c) no chemical reactions, (d) insignificant radioactive heat transfer, (e) insignificant viscous dissipation, (f) base fluid and nanoparticles regionally in thermal equilibrium.

Law of conservation of mass (Component form):

$$\frac{\partial \tilde{u}'}{\partial \tilde{\zeta}} + \frac{\partial \tilde{v}'}{\partial \tilde{\eta}} = 0. \quad (2.2)$$

Axial momentum equation:

$$\rho_{nf} \left(\frac{\partial}{\partial \tilde{t}} + \tilde{u}' \frac{\partial}{\partial \tilde{\zeta}} + \tilde{v}' \frac{\partial}{\partial \tilde{\eta}} \right) \tilde{u}' = -\frac{\partial \tilde{p}'}{\partial \tilde{\zeta}} + \mu_{nf} \left(\frac{\partial^2 \tilde{u}'}{\partial \tilde{\zeta}^2} + \frac{\partial^2 \tilde{u}'}{\partial \tilde{\eta}^2} \right) + g (\rho \gamma)_{nf} (\tilde{T}' - \tilde{T}_1). \quad (2.3)$$

Transverse momentum equation:

$$\rho_{nf} \left(\frac{\partial}{\partial \tilde{t}} + \tilde{u}' \frac{\partial}{\partial \tilde{\zeta}} + \tilde{v}' \frac{\partial}{\partial \tilde{\eta}} \right) \tilde{v}' = -\frac{\partial \tilde{p}'}{\partial \tilde{\eta}} + \mu_{nf} \left(\frac{\partial^2 \tilde{v}'}{\partial \tilde{\zeta}^2} + \frac{\partial^2 \tilde{v}'}{\partial \tilde{\eta}^2} \right). \quad (2.4)$$

Energy equation:

$$(\rho c_p)_{nf} \left(\frac{\partial}{\partial \tilde{t}} + \tilde{u}' \frac{\partial}{\partial \tilde{\zeta}} + \tilde{v}' \frac{\partial}{\partial \tilde{\eta}} \right) \tilde{T}' = k_{nf} \left(\frac{\partial^2 \tilde{T}'}{\partial \tilde{\zeta}^2} + \frac{\partial^2 \tilde{T}'}{\partial \tilde{\eta}^2} \right) + \tilde{Q}_0. \quad (2.5)$$

In above equations; \tilde{u}' and \tilde{v}' represents axial and transverse velocities, $\tilde{\eta}$ transverse coordinate, \tilde{T}' shows temperature, \tilde{T}_1 is wall temperature, \tilde{Q}_0 is constant heat absorption parameter, g denotes gravity, ρ_{nf} depicts density of nanofluids, k_f denotes thermal conductivity of the base fluid, \tilde{p}' denotes pressure, γ_{nf} depicts the thermal expansion coefficient. Moreover $(\rho c_p)_{nf}$ represents heat capacitance.

To non-dimensionlize the BVP, the given non-dimensional parameters are used as described in Eq. (2.6)

$$\xi = \frac{\tilde{\zeta}}{\lambda}, \eta = \frac{\tilde{\eta}}{a_0}, t = \frac{c\tilde{t}}{\lambda}, u = \frac{\tilde{u}'}{c}, v = \frac{\tilde{v}'}{c\delta}, p = \frac{\tilde{p}'a_0^2}{\mu c \lambda}, h = \frac{\tilde{h}}{a_0} = 1 + \frac{\alpha \xi}{\delta} - \varepsilon \cos \pi(\xi - t), \quad (2.6)$$

$$\delta = \frac{a_0}{\lambda}, \varphi = \frac{b}{a_0}, \theta = \frac{\tilde{T}' - \tilde{T}_1}{\tilde{T}_1}, \text{Re} = \frac{\rho_f c a_0}{\mu_f}, Gr_T = \frac{g \gamma_f \rho_f a_0^3 \tilde{T}_1}{\nu_f^2}, \beta = \frac{\tilde{Q}_0 a_0}{k_f \tilde{T}_1}.$$

Where θ is dimensionless temperature, δ is non-dimensional wave number, φ is rescaled nanoparticle volume fraction, ν is kinematic viscosity, ε is amplitude ratio, Re is Reynolds

number, β is heat absorption parameter and Gr_T is thermal Grashof number. By using long wavelength estimation (i.e. $\lambda > a$), it follows that $\delta \rightarrow 0$ and then also $Re \rightarrow 0$. By using these estimations, Equations (2.2) – (2.5) implies that:

$$\frac{\partial u}{\partial \xi} + \frac{\partial v}{\partial \eta} = 0, \quad (2.7)$$

$$\frac{\partial p}{\partial \xi} = \frac{\mu_{nf}}{\mu_f} \frac{\partial^2 u}{\partial \eta^2} + Gr_T \frac{(\rho\gamma)_{nf}}{(\rho\gamma)_f} \theta, \quad (2.8)$$

$$\frac{\partial p}{\partial \eta} = 0, \quad (2.9)$$

$$\frac{\partial^2 \theta}{\partial \eta^2} + \beta \frac{k_f}{k_{nf}} = 0. \quad (2.10)$$

The related boundary conditions are described as follows:

$$\left. \frac{\partial \theta}{\partial \eta}(\xi, \eta, t) \right|_{\eta=0} = 0, \theta(\xi, \eta, t) \Big|_{\eta=h} = 0, \quad (2.11)$$

$$\left. \frac{\partial u}{\partial \eta}(\xi, \eta, t) \right|_{\eta=0} = 0, u(\xi, \eta, t) \Big|_{\eta=h} = 0, \quad (2.12)$$

$$v(\xi, \eta, t) \Big|_{\eta=0} = 0, v(\xi, \eta, t) \Big|_{\eta=h} = \frac{\partial h}{\partial t}, \quad (2.13)$$

$$p \Big|_{\xi=0} = p_0, p \Big|_{\xi=l} = p_l. \quad (2.14)$$

The properties of the nanofluids Ref: [13] are described by:

$$(\rho\gamma)_{nf} = (1 - \varphi)(\rho\gamma)_f + \varphi(\rho\gamma)_s, \mu_{nf} = \frac{\mu_f}{(1 - \varphi)^{2.5}}, \quad (2.15a)$$

$$k_{nf} = k_f \left(\frac{(1 - \varphi) + \frac{2\varphi k_{CNT}}{k_{CNT} - k_f} \log\left(\frac{k_{CNT} + k_f}{2k_f}\right)}{(1 - \varphi) + \frac{2\varphi k_f}{k_{CNT} - k_f} \log\left(\frac{k_{CNT} + k_f}{2k_f}\right)} \right). \quad (2.15b)$$

Here ρ_f denotes fluid density, ρ_s represents density of the nanoparticles, k_{CNT} denotes

thermal conductivity of the SWCnt and MWCnt, γ_f represents the thermal expansion coefficient of base fluid, γ_s denotes the thermal expansion coefficient of the nanoparticles and φ represents the nanoparticle volume fraction.

2.3. Analytical solutions:

The mathematical solutions of above Eqs. (2.8) – (2.10) are obtained as:

$$\theta(\xi, \eta, t) = \frac{1}{2} \left[\frac{k_f}{k_{nf}} \beta (h - \eta)(h + \eta) \right], \quad (2.16)$$

$$u(\xi, \eta, t) = \frac{(\eta^2 - h^2) \left\{ \frac{k_f}{k_{nf}} \beta Gr_T \frac{(\rho\gamma)_{nf}}{(\rho\gamma)_f} (\eta^2 - 5h^2) \right\} + 12 \frac{dP}{d\xi}}{24(1-\varphi)^{-2.5}}. \quad (2.17)$$

To calculate transverse velocity, the axial velocity equation (2.17) along with boundary condition (2.13) is used in equation (2.7). The expression for transverse velocity becomes:

$$v(\xi, \eta, t) = \frac{\eta h \frac{\partial h}{\partial \xi} \left(\frac{k_f}{k_{nf}} \beta Gr_T \frac{(\rho\gamma)_{nf}}{(\rho\gamma)_f} (\eta^2 - 5h^2) + 6 \frac{dP}{d\xi} \right) - \eta (\eta^2 - 3h^2) \frac{d^2 P}{d\xi^2}}{6(1-\varphi)^{-2.5}}. \quad (2.18)$$

By using vibration transverse boundary condition in Eq. (2.18) gives :

$$(1 - \varphi)^{-2.5} \frac{\partial h}{\partial t} = \frac{\partial h}{\partial \xi} \left(\frac{k_f}{k_{nf}} \beta Gr_T \frac{(\rho\gamma)_{nf}}{(\rho\gamma)_f} \left(-\frac{2}{3} h^4 \right) + h^2 \frac{dP}{d\xi} \right) + \frac{h^3}{3} \frac{d^2 P}{d\xi^2}. \quad (2.19)$$

To calculate pressure gradient, Integrate Eq. (2.19) w.r.t. ξ :

$$\frac{\partial P}{\partial \xi} = \frac{3}{h^3} \left\{ A(t) + \frac{\epsilon \cos \pi(\xi - t)}{(1-\varphi)^{2.5}} \right\} + Gr_T \frac{(\rho\gamma)_{nf}}{(\rho\gamma)_f} \left(\frac{2}{5} \frac{k_f}{k_{nf}} \beta h^2 \right). \quad (2.20)$$

To calculate pressure difference ΔP , Integrate (2.20) w.r.t. ξ :

$$\Delta P(\xi, t) = \int_0^\xi \frac{3}{h^3} \left\{ A(t) + \frac{\epsilon \cos \pi(\xi - t)}{(1-\varphi)^{2.5}} \right\} + Gr_T \frac{(\rho\gamma)_{nf}}{(\rho\gamma)_f} \left(\frac{2}{5} \frac{k_f}{k_{nf}} \beta h^2 \right) d\xi. \quad (2.21)$$

Upon replacing $\Delta P(\xi, t) = p(\xi, t) - p(0, t)$ and $\xi = l$, and putting the finite length condition, we get:

$$p_l - p_0 = \int_0^l \left\{ \frac{3}{h^3} \left\{ A(t) + \frac{\epsilon \cos \pi(\xi-t)}{(1-\phi)^{2.5}} \right\} + Gr_T \frac{(\rho\gamma)_{nf}}{(\rho\gamma)_f} \left(\frac{2}{5} \frac{k_f}{k_{nf}} \beta h^2 \right) \right\} d\xi . \quad (2.22)$$

Where $A(t)$ is calculated by re-arranging (2.22) and solving with the help of Mathematica, it gives :

$$A(t) = \frac{(p_l - p_0) - \int_0^l \left[\frac{3\epsilon \cos \pi(\xi-t)}{h^3(1-\phi)^{2.5}} \right] d\xi - Gr_T \frac{(\rho\gamma)_{nf}}{(\rho\gamma)_f} \left[\frac{2}{5} \frac{k_f}{k_{nf}} \beta \int_0^l h^2 d\xi \right]}{\int_0^l \frac{3}{h^3} d\xi} . \quad (2.23)$$

2.4. Graphical representation and discussion:

From figure 2.2, It is seen that the thermal conductivity gains higher magnitude for SWCnt as compared to MWCnt by providing each constraint a fixed value . From figure 2.3, It is seen that the temperature rise gains more magnitude and varies directly with β for an irregular channel. Moreover, the rise in temperature is slightly less for SWCnt's as compared to MWCnt's. From Fig. 2.4, we observe that by increasing both β and Gr_T , the axial velocity $u(\xi, \eta)$ increases. The axial velocity for MWCnt is higher than SWCnt in all covers but this grow is slightly greater in case of regular channel and it is maximum where $\eta = 0$. Fig. 2.5 shows the transverse velocity and its diversification for β and Gr_T . Like axial velocity, the transverse velocity holds same amenities except that it is minimum where $\eta = 0$. It is observed that MWCnt's play their key role to increase the magnitude of both transverse and axial velocities. Fig. 2.6 depicts the sinusoidal behaviour of Pressure gradient. Pressure gradient and thermal Grashof number are directly in relation. For $\alpha \neq 0$ (i.e.non-uniform channel), by increasing the channel's length the pressure gradient increases.

For both SWCnt and MWCnt, the streamlines are drawn for distinct values of β as depicted in figures 2.7 and 2.8(a,b). Graphs show that in the case of SWCnt bolus decreases in size and increases in number by increasing β . But for MWCnt, we have opposite results. The size of trapped bolus increases and bolus decreases in number by increasing β . In both cases (i.e. SWCnt and MWCnt), streamlines for various values of Gr_T are shown in Figs. 2.9 and 2.10(a,b). It is noted that with an increase of Gr_T (for SWCnt and MWCnt), the size of trapped bolus decreases.

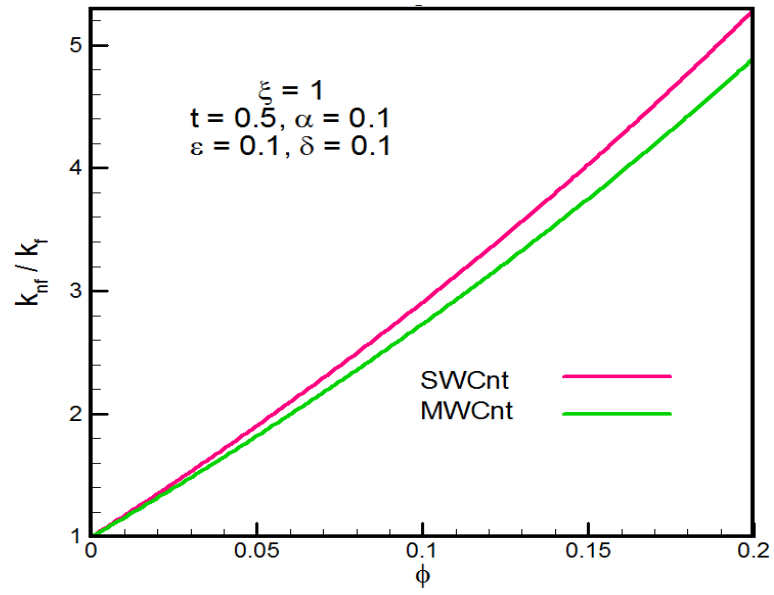


Fig. 2.2 Effective thermal conductivity ($\frac{k_{nf}}{k_f}$).

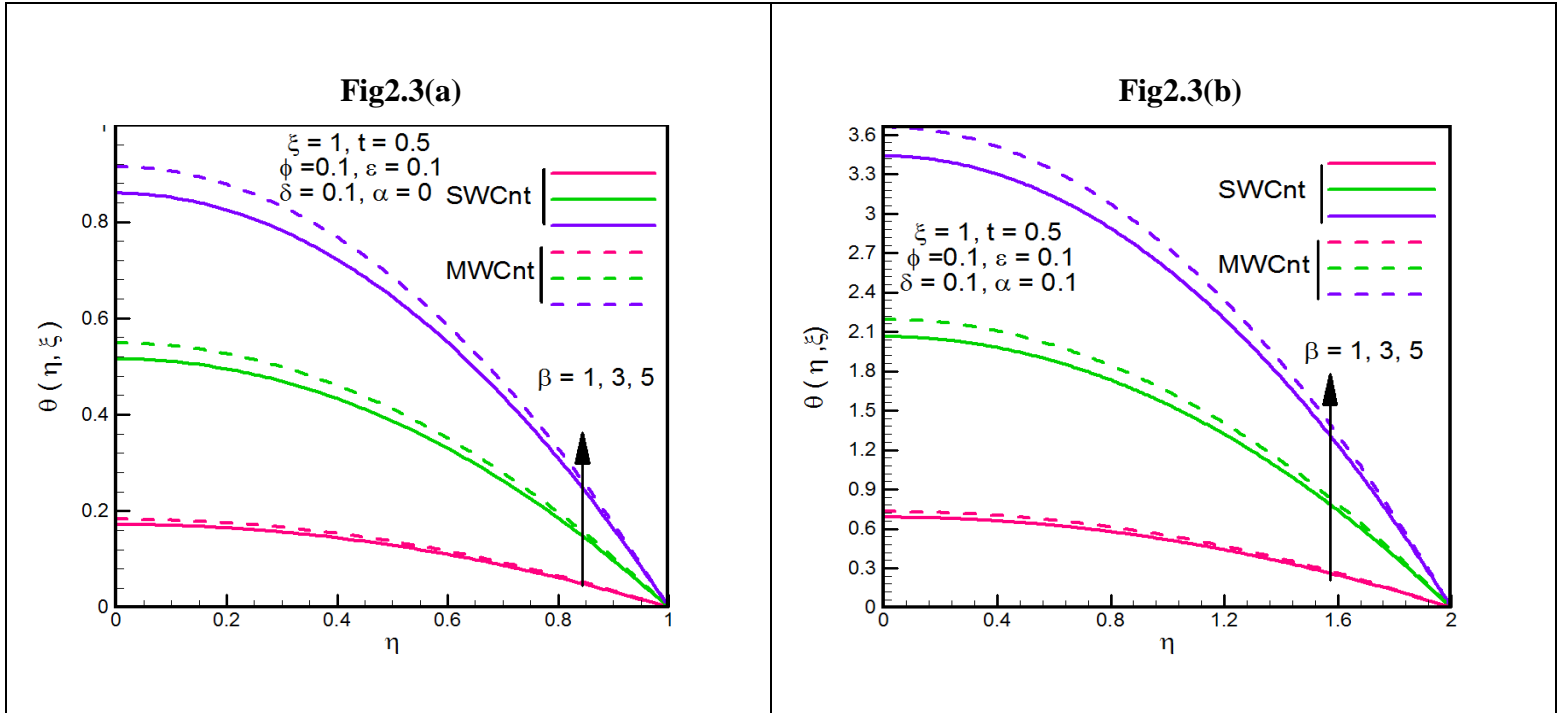


Fig. 2.3 Temperature profile ($\theta(\xi, \eta)$ vs η) for various values of (a) β where $\alpha = 0$, (b) β where $\alpha = 0.1$.

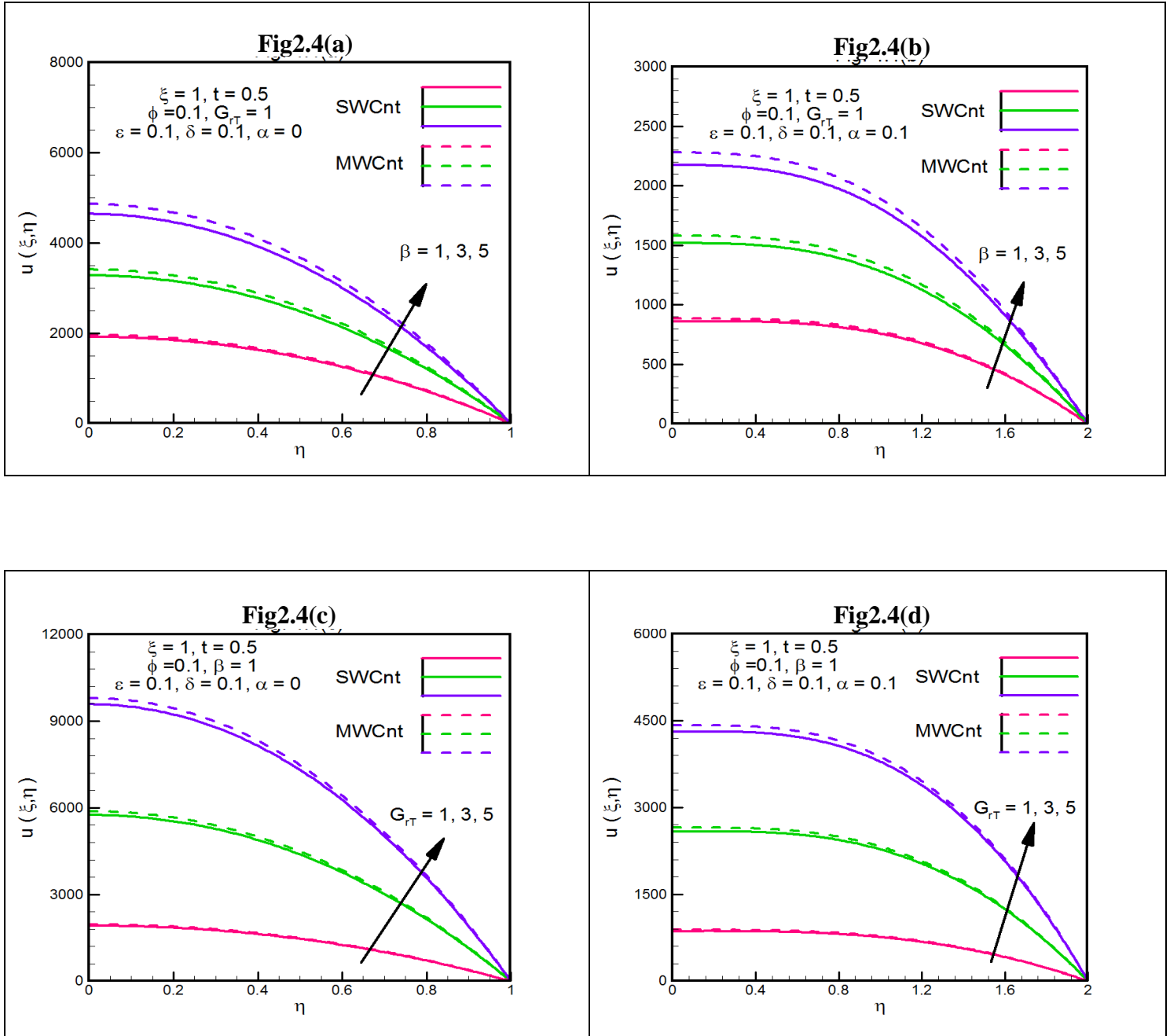


Fig. 2.4 Axial velocity profile ($u(\xi, \eta)$ vs η) for various values of (a) β where $\alpha = 0$, (b) β where $\alpha = 0.1$, (c) Gr_T where $\alpha = 0$, (d) Gr_T where $\alpha = 0.1$.

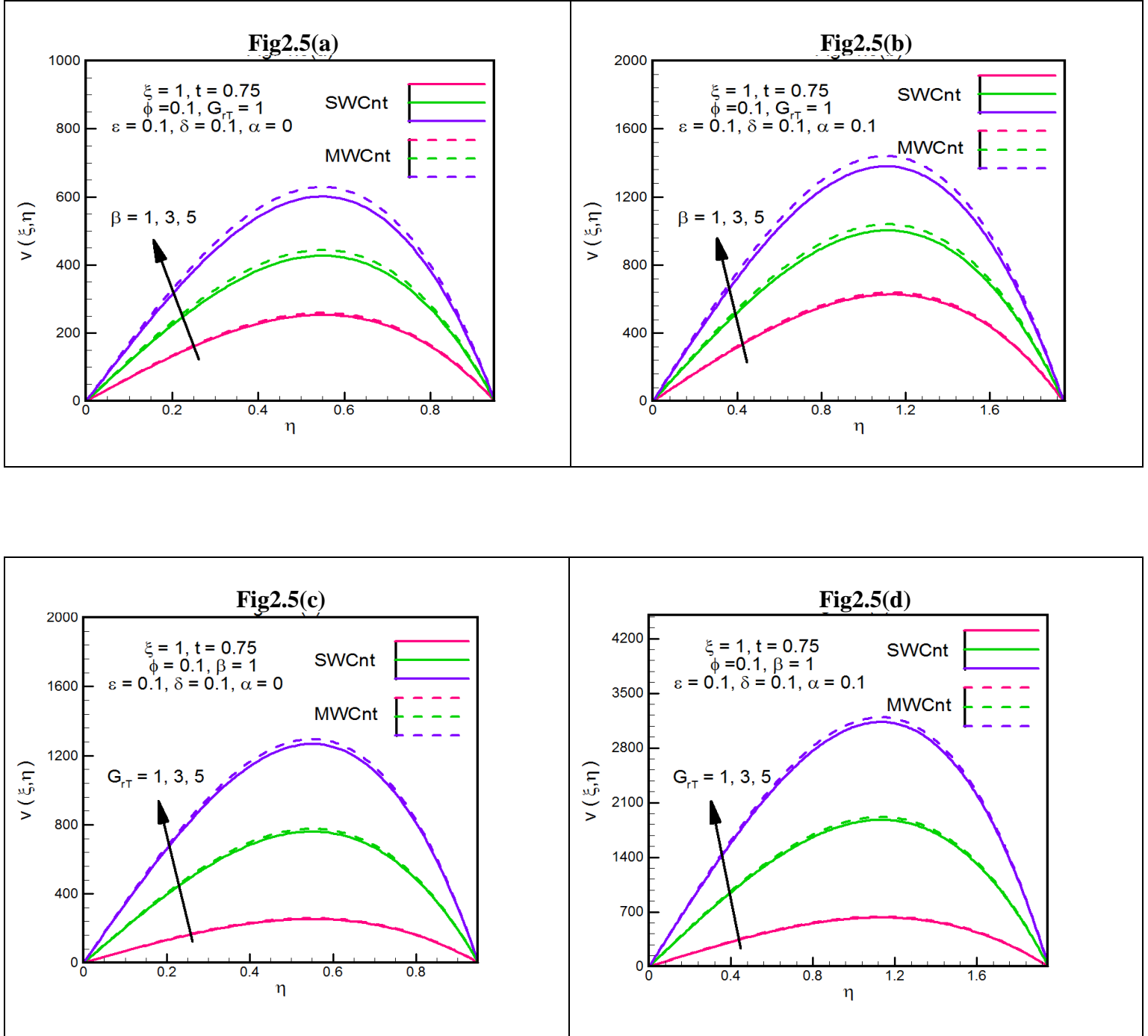


Fig. 2.5 Transverse velocity profile ($v(\xi, \eta)$ vs η) for various values of (a) β where $\alpha = 0$, (b) β where $\alpha = 0.1$, (c) Gr_T where $\alpha = 0$, (d) Gr_T where $\alpha = 0.1$.

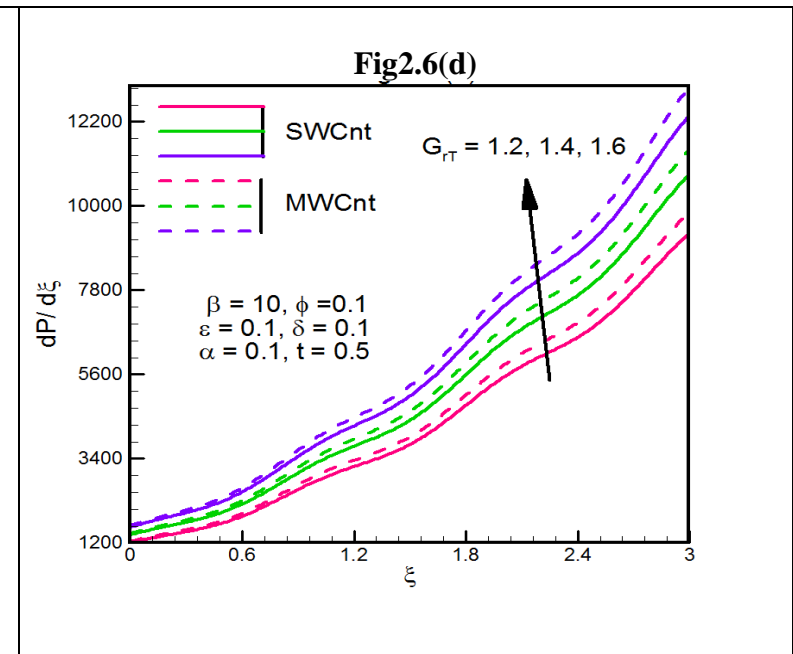
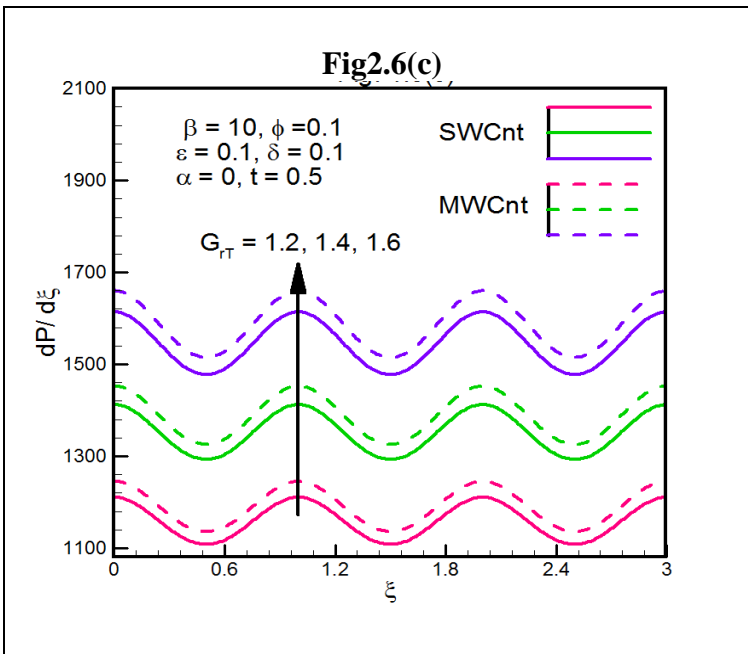
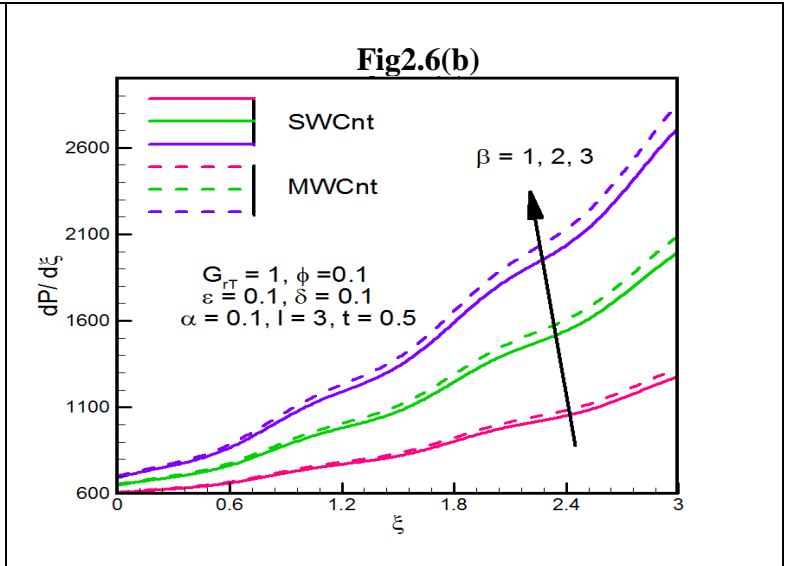
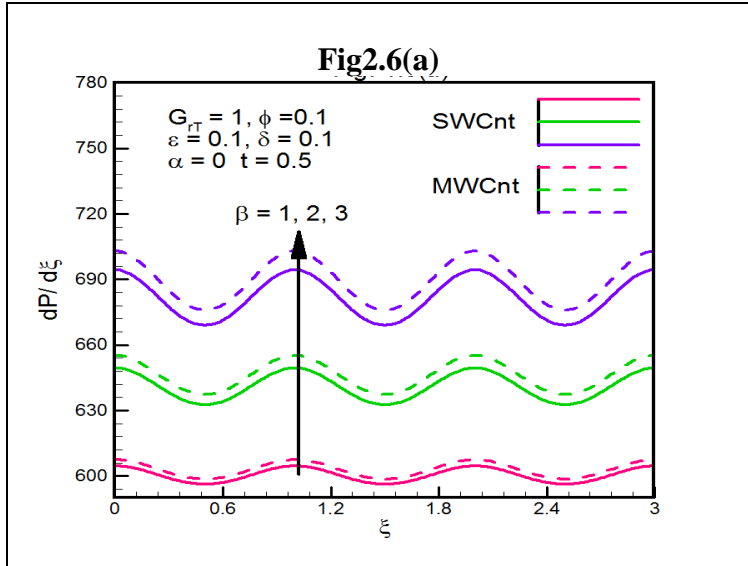
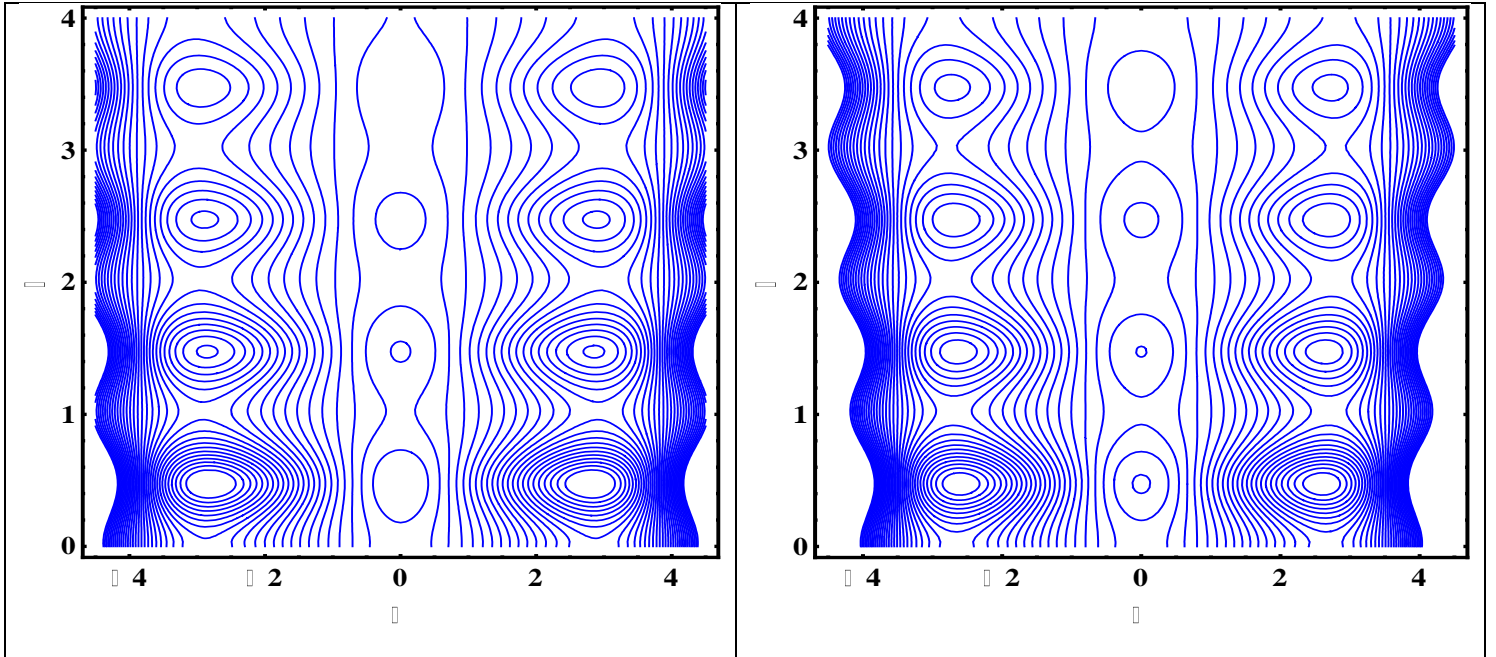
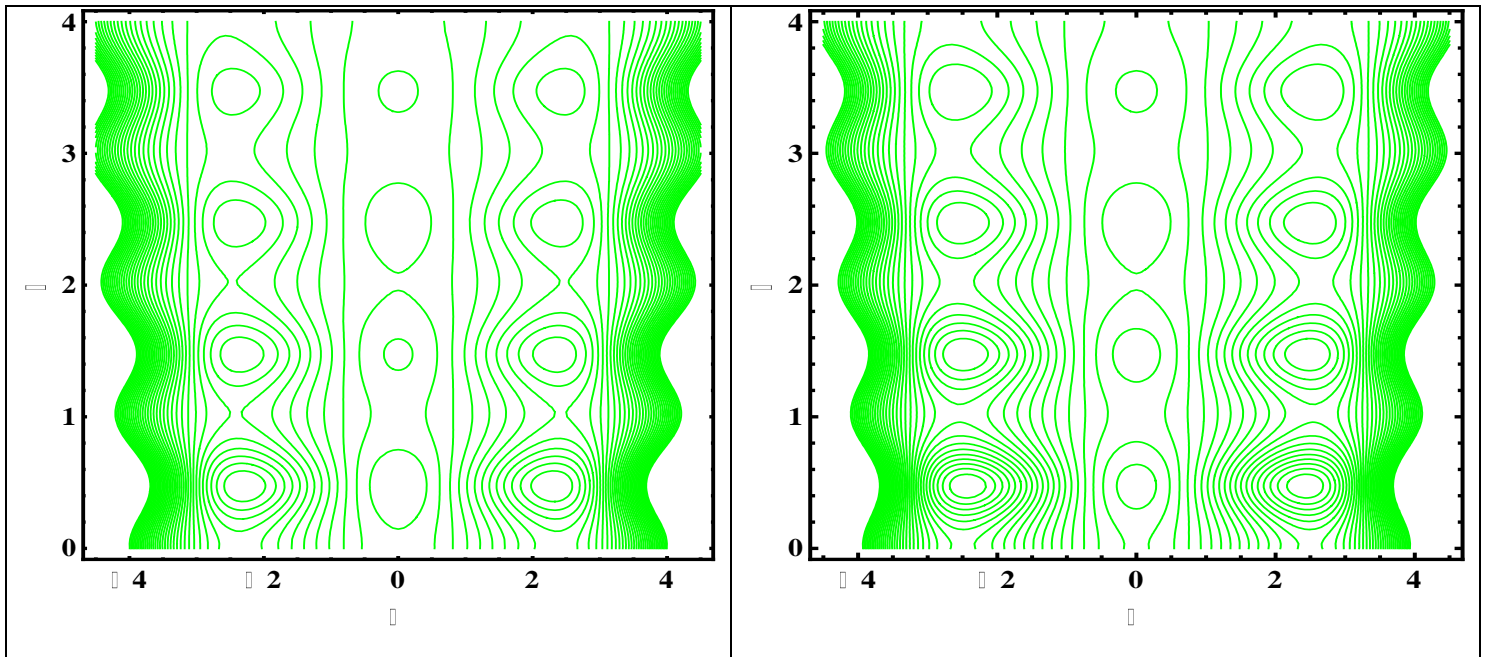


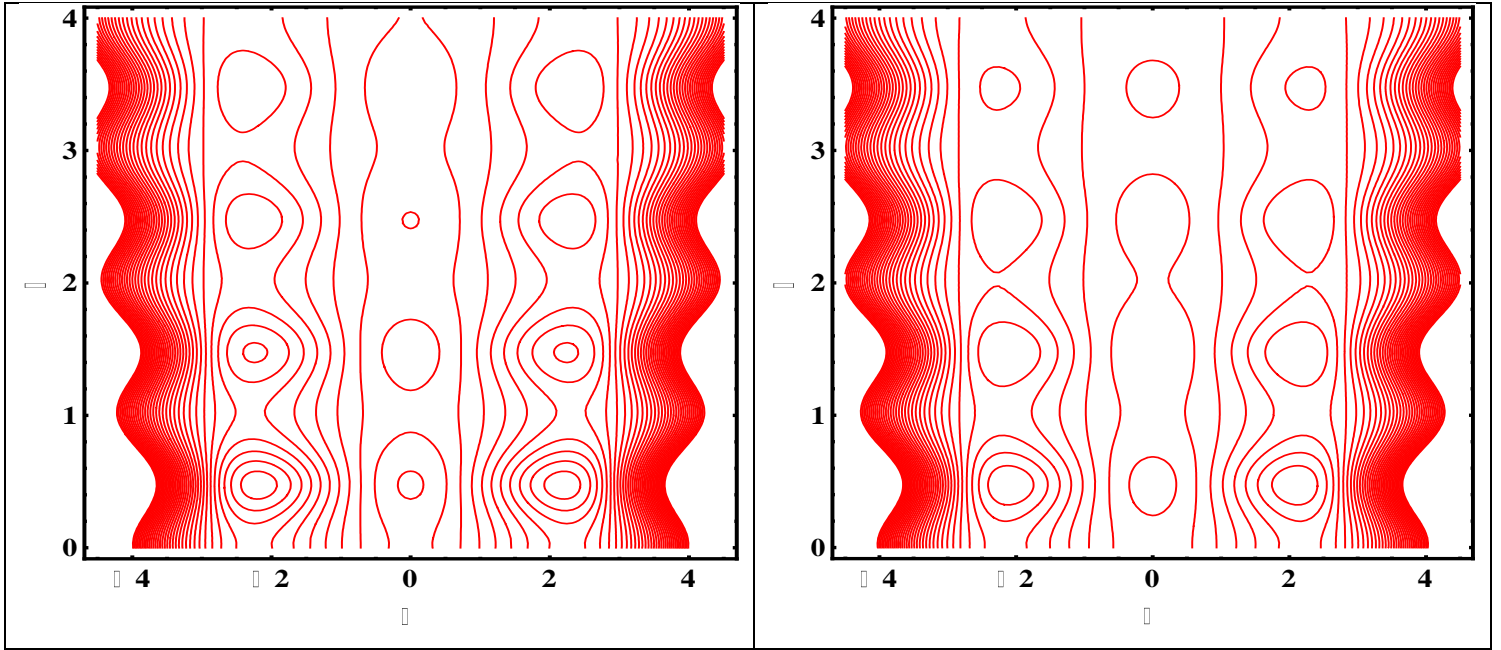
Fig. 2.6 Pressure gradient for discrete values of (a) β where $\alpha = 0$, (b) β where $\alpha = 0.1$, (c) Gr_T where $\alpha = 0$, (d) Gr_T where $\alpha = 0.1$.



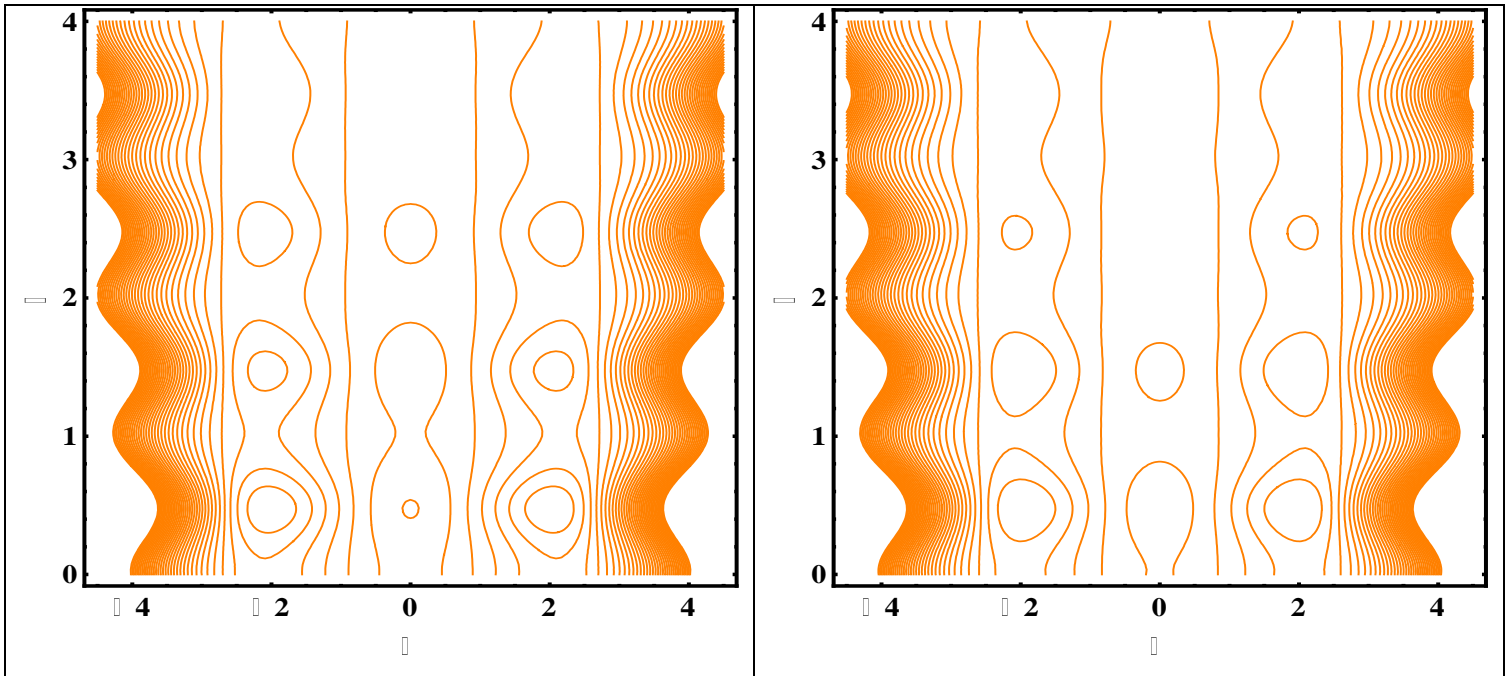
Figs. 2.7 Streamlines (SWCnt) for (a) $\beta = 0.5$. (b) $\beta = 0.8$. Other constants are $Gr_T = 0.5$, $\phi=0.2$, $\alpha=0.4$, $\varepsilon = 0.3$, $t=0.5$, $\delta = 0.1$.



Figs. 2.8 Streamlines (MWCnt) for (a) $\beta = 0.5$. (b) $\beta = 0.8$. Other constants are $Gr_T = 0.5$, $\phi=0.2$, $\alpha=0.4$, $\varepsilon = 0.3$, $t=0.5$, $\delta = 0.1$.



Figs.2.9 Streamlines (SWCnt) for (a) $Gr_T = 0.3$. (b) $Gr_T = 0.6$. Other constants are $\beta=0.5$, $\phi=0.2$, $\alpha=0.4$, $\epsilon=0.3$, $t=0.5$, $\delta=0.1$.



Figs 2.10 Streamlines (MWCnt) for (a) $Gr_T = 0.3$. (b) $Gr_T = 0.6$. Other constants are $\beta = 0.5$, $\phi=0.2$, $\alpha=0.4$, $\epsilon=0.3$, $t=0.5$, $\delta=0.1$.

2.5. Conclusions:

1. The temperature rise is greater for MWCnt.
2. Axial velocity increases by increasing both β and Gr_T .
3. The pressure gradient rises by increasing both β and Gr_T .
4. By increasing the values of β and Gr_T , the pressure difference reduces.
5. By increasing β for SWCnt, the trapped bolus increases in number and decreases in size.
6. By increasing β for MWCnt, the trapped bolus decreases in number and decreases in size.
7. By increasing values of Gr_T , size of boluses decreases for both SWCnt and MWCnt.

Chapter 3

Pressure Driven Peristaltic Flow Study With the Interaction of Nanoparticles

3.1. Introduction:

In this chapter an analytical investigation of Carbon nanotubes(CNTs) with variable viscosity is done to analyse the peristaltic transient flow of nanofluids in an irregular pipe of finite measure. This flow geometry accommodates a broad range of biological applications. Exact mathematical solutions are determined. Influence of CNTs on temperature, axial and transverse velocities, effective thermal conductivity and on pressure gradient is studied graphically. Trapping is also studied. The model has applications in drugs delivery system.

3.2. Mathematical formulation:

The geometrical model is same as it was taken in chapter 2 which is given in Eq(2.1). Governing equations are amended with low-Reynolds number and also long wavelength approximation is taken into account. T_1 denotes the extent of the temperature at the wall ($\eta = h$). According to Boussinesq interpretation, the transport equations with a particular reference pressure are described in Ref: [35] for the scheme and subsequent assumptions are considered as: (a) Streamline flow with constant density, (b) negligible external forces, (c) no chemical reactions, (d) insignificant radioactive heat transfer, (e) insignificant viscous dissipation, (f) base fluid and nanoparticles regionally in thermal equilibrium, (g) variable fluid viscosity is considered.

Law of conservation of mass (Component form):

$$\frac{\partial \tilde{u}'}{\partial \tilde{\zeta}} + \frac{\partial \tilde{v}'}{\partial \tilde{\eta}} = 0. \quad (3.1)$$

Axial momentum equation:

$$\rho_{nf} \left(\frac{\partial}{\partial \tilde{t}} + \tilde{u}' \frac{\partial}{\partial \tilde{\zeta}} + \tilde{v}' \frac{\partial}{\partial \tilde{\eta}} \right) \tilde{u}' = - \frac{\partial \tilde{p}'}{\partial \tilde{\zeta}} + \mu_{nf} \left(\frac{\partial^2 \tilde{u}'}{\partial \tilde{\zeta}^2} + \frac{\partial^2 \tilde{u}'}{\partial \tilde{\eta}^2} \right) + g (\rho \gamma)_{nf} (\tilde{T}' - \tilde{T}_1). \quad (3.2)$$

Transverse momentum equation:

$$\rho_{nf} \left(\frac{\partial}{\partial \tilde{t}} + \tilde{u}' \frac{\partial}{\partial \tilde{\zeta}} + \tilde{v}' \frac{\partial}{\partial \tilde{\eta}} \right) \tilde{v}' = - \frac{\partial \tilde{p}'}{\partial \tilde{\eta}} + \mu_{nf} \left(\frac{\partial^2 \tilde{v}'}{\partial \tilde{\zeta}^2} + \frac{\partial^2 \tilde{v}'}{\partial \tilde{\eta}^2} \right). \quad (3.3)$$

Energy equation:

$$(\rho c_p)_{nf} \left(\frac{\partial}{\partial \tilde{t}} + \tilde{u}' \frac{\partial}{\partial \tilde{\zeta}} + \tilde{v}' \frac{\partial}{\partial \tilde{\eta}} \right) \tilde{T}' = k_{nf} \left(\frac{\partial^2 \tilde{T}'}{\partial \tilde{\zeta}^2} + \frac{\partial^2 \tilde{T}'}{\partial \tilde{\eta}^2} \right) + \tilde{Q}_0. \quad (3.4)$$

Here \tilde{u}' and \tilde{v}' represents axial and transverse velocities, $\tilde{\eta}$ transverse coordinate, \tilde{T}' shows temperature, \tilde{T}_1 is wall temperature, \tilde{Q}_0 is constant heat absorption parameter, g denotes gravity, ρ_{nf} depicts density of nanofluids, k_f denotes thermal conductivity of the base fluid, \tilde{p}' denotes pressure, γ_{nf} depicts the thermal expansion coefficient. Moreover $(\rho c_p)_{nf}$ represents heat capacitance.

To non-dimensionalize the BVP, the given non-dimensional parameters are used as described in Eq. (3.5).

$$\begin{aligned} \xi = \frac{\tilde{\zeta}}{\lambda}, \eta = \frac{\tilde{\eta}}{a_0}, t = \frac{c \tilde{t}}{\lambda}, u = \frac{\tilde{u}'}{c}, v = \frac{\tilde{v}'}{c \delta}, p = \frac{\tilde{p}' a_0^2}{\mu c \lambda}, h = \frac{\tilde{h}}{a_0} = 1 + \frac{\alpha \xi}{\delta} - \varepsilon \cos \pi(\xi - t), \\ \delta = \frac{a_0}{\lambda}, \varphi = \frac{b}{a_0}, \theta = \frac{\tilde{T}' - \tilde{T}_1}{\tilde{T}_1}, \text{Re} = \frac{\rho_f c a_0}{\mu_f}, Gr_T = \frac{g \gamma_f \rho_f a_0^3 \tilde{T}_1}{\nu_f^2}, \beta = \frac{\tilde{Q}_0 a_0}{k_f \tilde{T}_1}. \end{aligned} \quad (3.5)$$

Where δ is dimensionless wave number, ν is kinematic viscosity, ε is amplitude ratio, φ is rescaled nanoparticle volume fraction, θ is dimensionless temperature, Re is Reynolds number, β is heat absorption parameter and Gr_T is thermal Grashof number. By using long wavelength estimation (i.e. the wavelength for peristaltic is much more than the channel breadth, viz, $\lambda > a$), As $\delta \rightarrow 0$ and then also $\text{Re} \rightarrow 0$. Intending $\delta \rightarrow 0$ refutes channel curvature effects and convective inertial forces are neutralised in comparison of viscous

hydrodynamic forces as $Re \rightarrow 0$. By using these estimations, Equations (3.1) – (3.4) implies that:

$$\frac{\partial u}{\partial \xi} + \frac{\partial v}{\partial \eta} = 0, \quad (3.6)$$

$$\frac{\partial p}{\partial \xi} = \frac{\partial}{\partial \eta} \left(\frac{\mu_{nf}}{\mu_f} \frac{\partial u}{\partial \eta} \right) + Gr_T \frac{(\rho\gamma)_{nf}}{(\rho\gamma)_f} \theta, \quad (3.7)$$

$$\frac{\partial p}{\partial \eta} = 0, \quad (3.8)$$

$$\frac{\partial^2 \theta}{\partial \eta^2} + \beta \frac{k_f}{k_{nf}} = 0. \quad (3.9)$$

The related boundary conditions are described as follows:

$$\left. \frac{\partial \theta}{\partial \eta}(\xi, \eta, t) \right|_{\eta=0} = 0, \theta(\xi, \eta, t) \Big|_{\eta=h} = 0, \quad (3.10)$$

$$\left. \frac{\partial u}{\partial \eta}(\xi, \eta, t) \right|_{\eta=0} = 0, u(\xi, \eta, t) \Big|_{\eta=h} = 0, \quad (3.11)$$

$$v(\xi, \eta, t) \Big|_{\eta=0} = 0, v(\xi, \eta, t) \Big|_{\eta=h} = \frac{\partial h}{\partial t}, \quad (3.12)$$

$$p \Big|_{\xi=0} = p_0, p \Big|_{\xi=l} = p_l. \quad (3.13)$$

The properties of the nanofluids Ref: [13] are described by:

$$(\rho\gamma)_{nf} = (1 - \phi)(\rho\gamma)_f + \phi(\rho\gamma)_s, k_{nf} = k_f \left(\frac{(1 - \phi) + \frac{2\phi k_{CNT}}{k_{CNT} - k_f} \log\left(\frac{k_{CNT} + k_f}{2k_f}\right)}{(1 - \phi) + \frac{2\phi k_f}{k_{CNT} - k_f} \log\left(\frac{k_{CNT} + k_f}{2k_f}\right)} \right). \quad (3.14)$$

The Reynold's model for nanofluid viscosity can be defined as follows:

$$\frac{\mu_{nf}}{\mu_f} = \frac{e^{-\alpha\theta}}{(1 - \phi)^{2.5}}, \text{ and } e^{-\alpha\theta} = 1 - \alpha\theta, \alpha \ll 1. \quad (3.15)$$

Where μ_f is constant viscosity of fluid and α is viscosity parameter.

In Eq(3.14), ρ_f represents fluid density, ρ_s denotes density of the nanoparticles, k_{CNT} represents thermal conductivity of the SWCnt and MWCnt, γ_f denotes the thermal expansion coefficient of base fluid, γ_s represents the thermal expansion coefficient of the nanoparticles and φ represents the nanoparticle volume fraction.

3.3. Analytical solutions:

The mathematical solutions of above Eqs. (3.7) – (3.9) are obtained as:

$$\theta(\xi, \eta, t) = \frac{1}{2} \left[\frac{k_f}{k_{nf}} \beta (h - \eta)(h + \eta) \right], \quad (3.16)$$

$$u(\xi, \eta, t) = \frac{(\eta^2 - h^2) \left\{ -\beta Gr_T \frac{k_f(\rho\gamma)_{nf}}{k_{nf}(\rho\gamma)_f} (\eta^2(-3 + \alpha\beta \frac{k_f}{k_{nf}} \eta^2) - 5h^2(-3 + \alpha\beta \frac{k_f}{k_{nf}} \eta^2) + 4\alpha\beta \frac{k_f}{k_{nf}} h^4) + 9(4 - \alpha\beta \frac{k_f}{k_{nf}} \eta^2 + \alpha\beta \frac{k_f}{k_{nf}} h^2) \frac{dP}{d\xi} \right\}}{72(1-\varphi)^{-2.5}}. \quad (3.17)$$

The expression for the transverse velocity in Eq.(3.18) is obtained by using the axial velocity given in (3.17) with boundary condition (3.12) in Eq.(3.6):

$$v(\xi, \eta, t) = \frac{-4\eta h \left\{ \beta Gr_T \frac{k_f(\rho\gamma)_{nf}}{k_{nf}(\rho\gamma)_f} (\eta^2(-5 + \alpha\beta \frac{k_f}{k_{nf}} \eta^2) + 5h^2(5 - \alpha\beta \frac{k_f}{k_{nf}} \eta^2 + 2\alpha\beta \frac{k_f}{k_{nf}} h^2)) + 5(-6 + \alpha\beta \frac{k_f}{k_{nf}} \eta^2 - 3\alpha\beta \frac{k_f}{k_{nf}} h^2) \frac{dP}{d\xi} \right\} \frac{\partial h}{\partial \xi} + \eta(\eta^2(-20 + 3\alpha\beta \frac{k_f}{k_{nf}} \eta^2) + 5h^2(12 - 2\alpha\beta \frac{k_f}{k_{nf}} \eta^2 + 3\alpha\beta \frac{k_f}{k_{nf}} h^2)) \frac{d^2 P}{d\xi^2}}{120(1-\varphi)^{-2.5}}. \quad (3.18)$$

The volume flow rate is defined as follows Ref: [25]:

$$Q = \int_0^h u d\eta. \quad (3.19)$$

By using Eq. (3.17) into Eq. (3.19), we get the following equation:

$$Q = \frac{Gr_T \frac{(\rho\gamma)_{nf}}{(\rho\gamma)_f} \frac{\beta k_f}{k_{nf}} h^5 (14 + 3\alpha \frac{\beta k_f}{k_{nf}} h^2) - 7h^3 (5 + \alpha \frac{\beta k_f}{k_{nf}} h^2) \frac{dP}{d\xi}}{105(1-\varphi)^{-2.5}}. \quad (3.20)$$

The wave frame (\tilde{X}, \tilde{Y}) is going with the velocity c , the transformation among a wave frame (\tilde{X}, \tilde{Y}) and the fixed frame $(\tilde{\xi}, \tilde{\eta})$ are considered as cited in Refs: [29-34]:

$$\tilde{X} = \tilde{\xi} - c\tilde{t}, \tilde{Y} = \tilde{\eta}, \tilde{U} = \tilde{u} - c, \tilde{V} = \tilde{v}, \quad (3.21)$$

Where (\tilde{U}, \tilde{V}) are the velocity components in the moving wave frame and (\tilde{u}, \tilde{v}) are the velocity components in the fixed frame respectively. The volume flow rate in wave frame can be calculated with the following relation:

$$Q = \int_0^h (U+1) dY. \quad (3.22)$$

By integrating Eq.(3.22),we get the following expression:

$$Q = q' + h \quad (3.23)$$

$$\text{Where } q' = \int_0^h U dY.$$

By taking the average volume flow rate through unit time period, we get:

$$\bar{Q} = \int_0^1 Q dt = \int_0^1 (q' + h) dt. \quad (3.24)$$

From Eq. (3.23) and Eq. (3.24), we obtained the following equation:

$$\bar{Q} = Q + 1 - h = q' + 1. \quad (3.25)$$

Eq. (3.20) and Eq. (3.25) yield a compressed form for the pressure gradient:

$$\frac{dp}{d\xi} = \frac{-105(1-\varphi)^{-2.5} (\bar{Q} - 1 + h) + Gr_T \frac{\beta k_f}{k_{nf}} \frac{(\rho\gamma)_{nf}}{(\rho\gamma)_f} h^5 (14 + 3 \frac{\alpha \beta k_f}{k_{nf}} h^2)}{7h^3 (5 + \frac{\alpha \beta k_f}{k_{nf}} h^2)}. \quad (3.26)$$

The pressure difference over unit wavelength (Δp) is given in Eq. (3.27) :

$$\Delta p = \int_0^1 \frac{dp}{d\xi} d\xi. \quad (3.27)$$

By applying the transformations of Eq. (3.21) into Eq. (3.17), the stream function in the wave frame (obeying the Cauchy–Riemann equations $U = \frac{\partial \psi}{\partial \eta}$, $V = -\frac{\partial \psi}{\partial \xi}$) is obtained as:

$$\psi(\xi, \eta) = \frac{Gr_T \beta \frac{k_f(\rho\gamma)_{nf}}{k_{nf}(\rho\gamma)_f} \eta (21\eta^4 - 5\alpha\beta \frac{k_f}{k_{nf}} \eta^6 + 7h^2(6\eta^2(-5 + \alpha\beta \frac{k_f}{k_{nf}} \eta^2) + 5h^2(15 - 3\alpha\beta \frac{k_f}{k_{nf}} \eta^2 + 4\alpha\beta \frac{k_f}{k_{nf}} h^2))) - 21\eta(\eta^2(-20 + 3\alpha\beta \frac{k_f}{k_{nf}} \eta^2) + 5h^2(12 - 2\alpha\beta \frac{k_f}{k_{nf}} \eta^2 + 3\alpha\beta \frac{k_f}{k_{nf}} h^2)) \frac{dP}{d\xi}}{2520(1-\varphi)^{-2.5}} - \eta. \quad (3.28)$$

3.4. Graphical representation and discussion:

From figure 3.1, It is seen that the thermal conductivity gains higher magnitude for SWCnt as compared to MWCnt by providing each constraint a fixed value . From figure 3.2(a,b), It is seen that the temperature rise gains more magnitude and varies directly with β for an irregular channel. Moreover, the rise in temperature is slightly less for SWCnt's as compared to MWCnt's.

Fig. 3.3(a,b,c,d) shows increase in axial velocity $u(\xi, \eta)$ by increasing β and Gr_T and the axial velocity for MWCnt is higher than that of SWCnt in both uniform and non-uniform channels but the velocity gains more magnitude for irregular pipe. Axial velocity is maximum at $\eta = 0$ which is actually the center of tube. The transverse velocity $v(\xi, \eta)$ and variation in it, for β and Gr_T is shown in Fig. 3.4(a-d). The transverse velocity by increasing both β and Gr_T in all cases but at the center of the tube where $\eta = 0$, it is minimum. It is noted that SWCnt achieves higher transverse velocity as compared to the MWCnt in both channels.

Fig. 3.5(a,b,c,d) presents that due to increase in β and Gr_T , pressure gradient increases and it shows linear behaviour. Pressure gradient is directly proportional to both β and Gr_T .

For both SWCnt and MWCnt, the streamlines for distinct values of β are shown in Figs. 3.6(a,b) and 3.7(a,b). Graphs show that with an increase in β for both SWCnt and MWCnt both the size and the number of bolus decreases.

Streamlines(SWCnt and MWCnt) for various values of Gr_T are shown in Figs. 3.8(a,b) and 3.9(a, b). It is perceived that with an increase in Gr_T , the trapped bolus decreases in number and size.

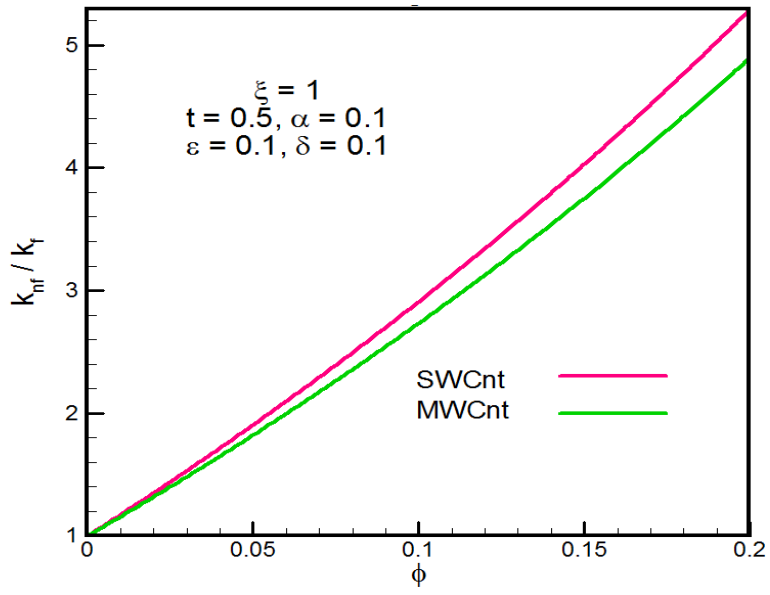


Fig. 3.1 Effective thermal conductivity ($\frac{k_{nf}}{k_f}$).

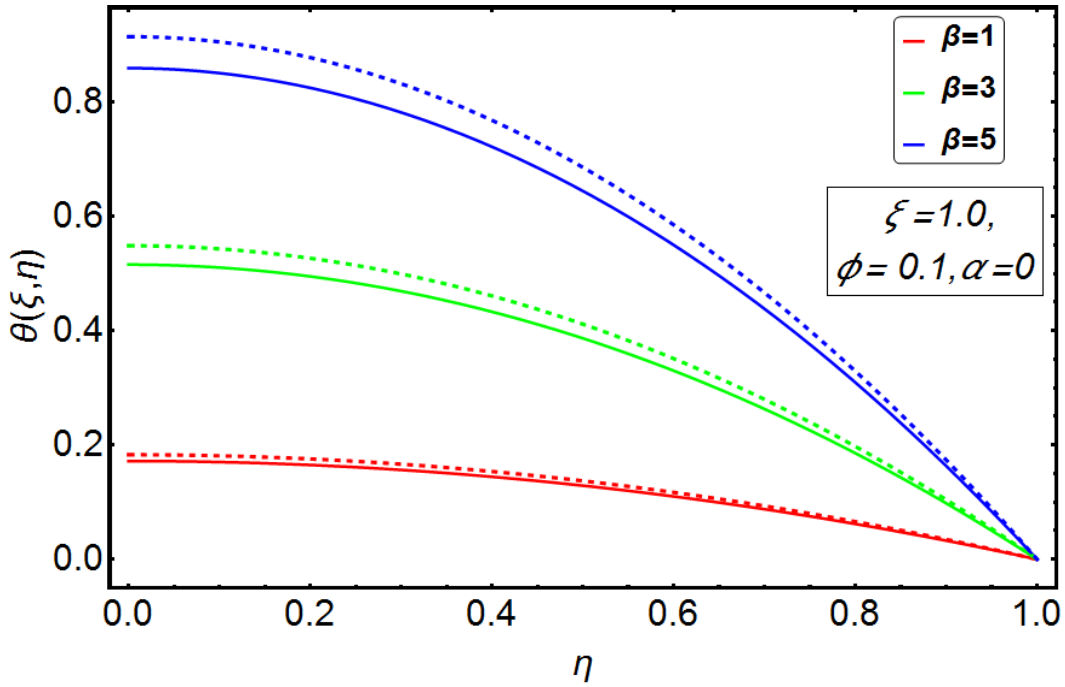


Fig. 3.2(a) Temperature profile ($\theta(\xi, \eta)$ vs η) for different values of β where $\alpha = 0$ (i.e. uniform channel).

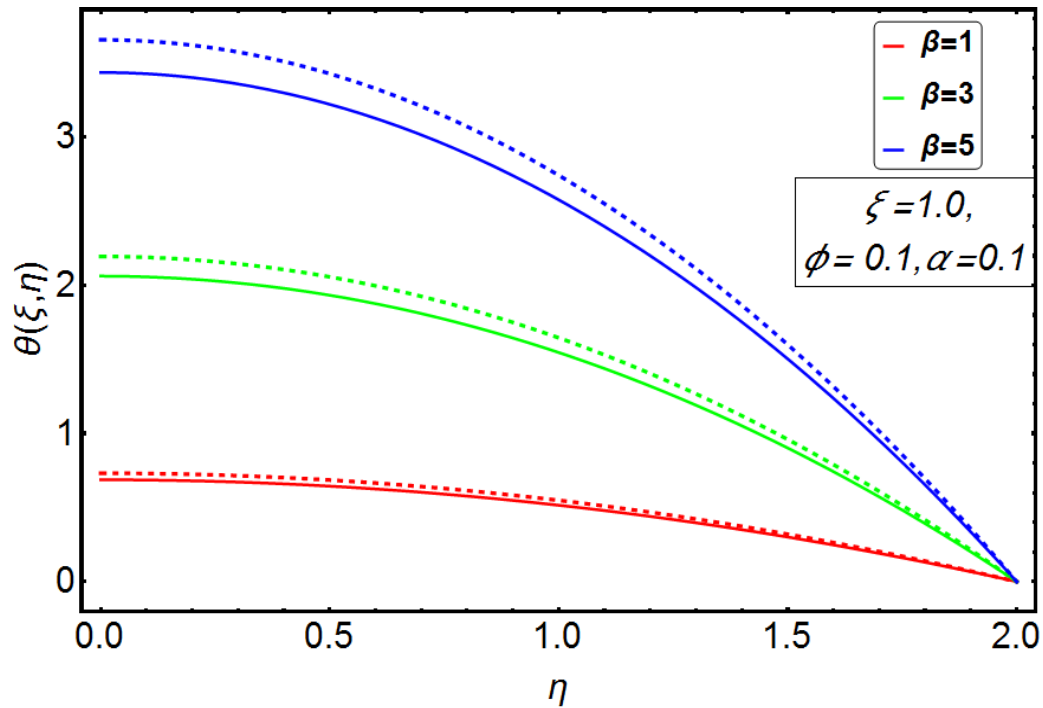


Fig. 3.2 (b) Temperature profile ($\theta(\xi, \eta)$ vs η) for different values of β where $\alpha = 0.1$ (i.e. non-uniform channel).

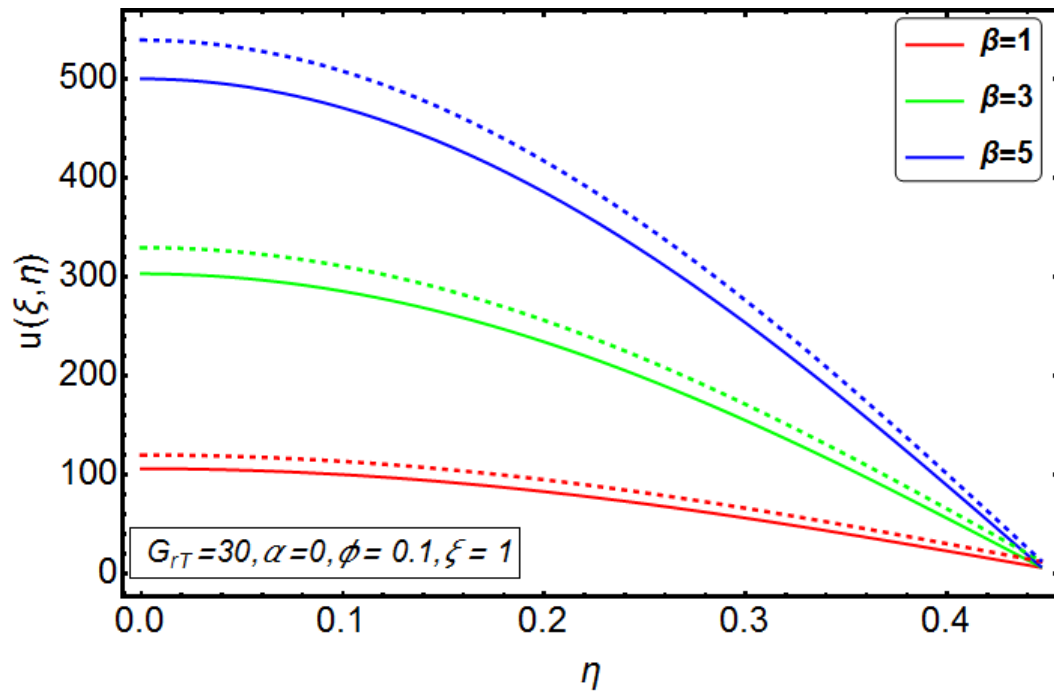


Fig. 3.3(a) Axial velocity profile ($u(\xi, \eta)$ vs η) for different values of β where $\alpha = 0$ (i.e. uniform channel).

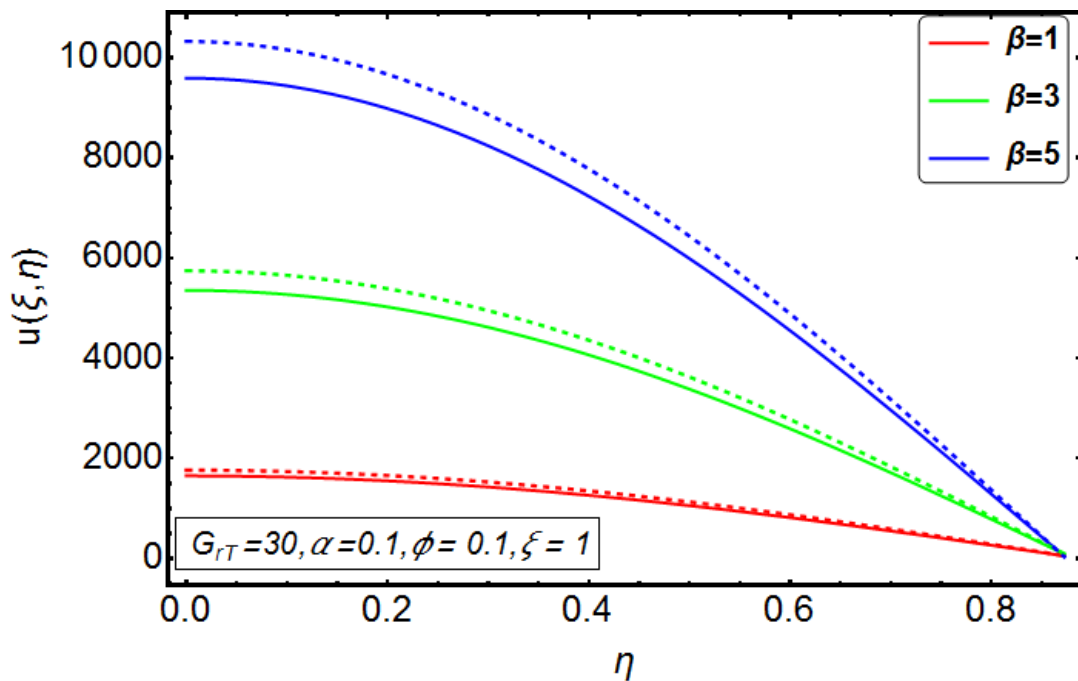


Fig. 3.3(b) Axial velocity profile ($u(\xi, \eta)$ vs η) for different values of β where $\alpha = 0.1$ (i.e. non-uniform channel).

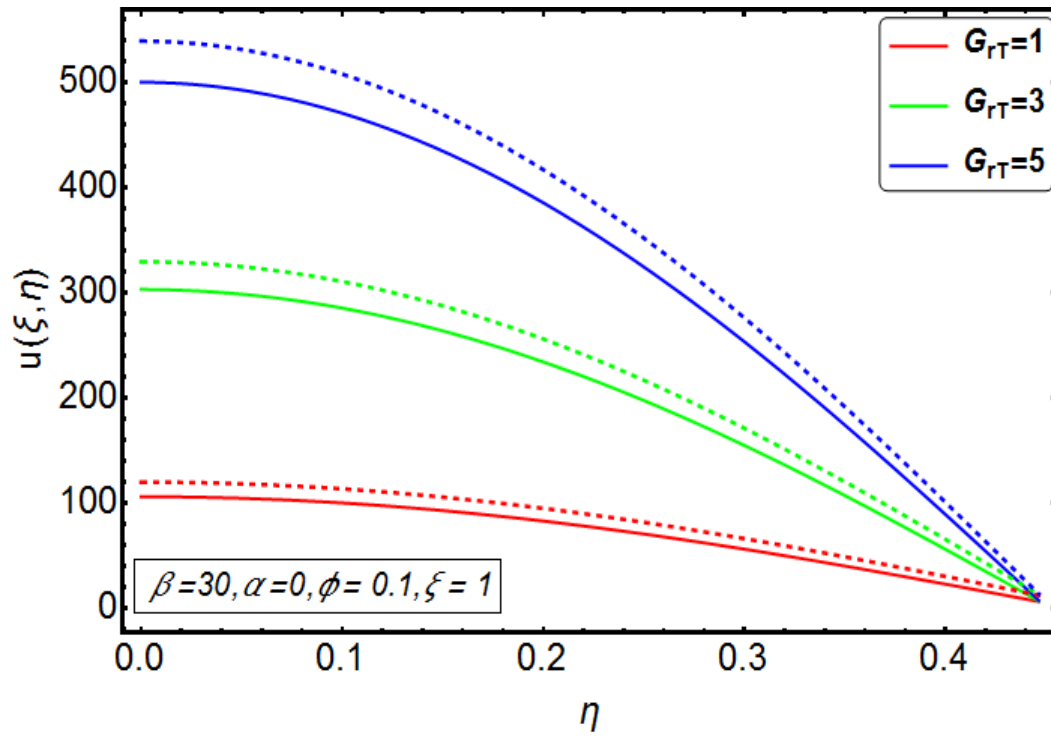


Fig. 3.3(c) Axial velocity profile ($u(\xi, \eta)$ vs η) for different values of Gr_T where $\alpha = 0$ (i.e. uniform channel).

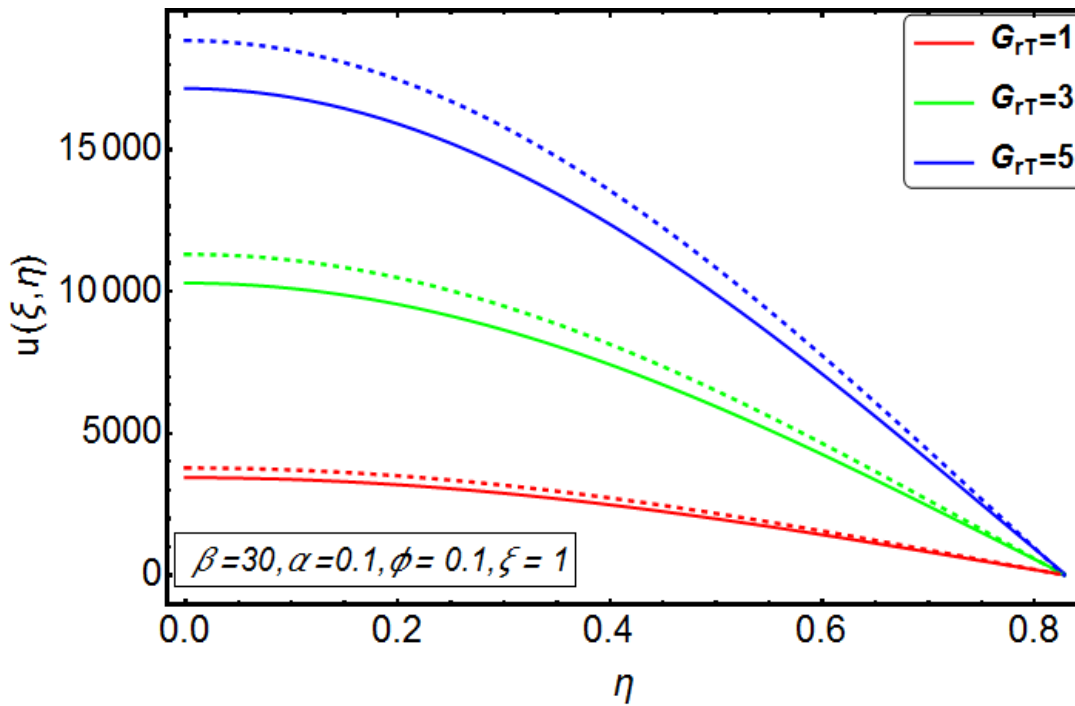


Fig. 3.3(d) Axial velocity profile ($u(\xi, \eta)$ vs η) for different values of Gr_T where $\alpha = 0.1$ (i.e. non-uniform channel).

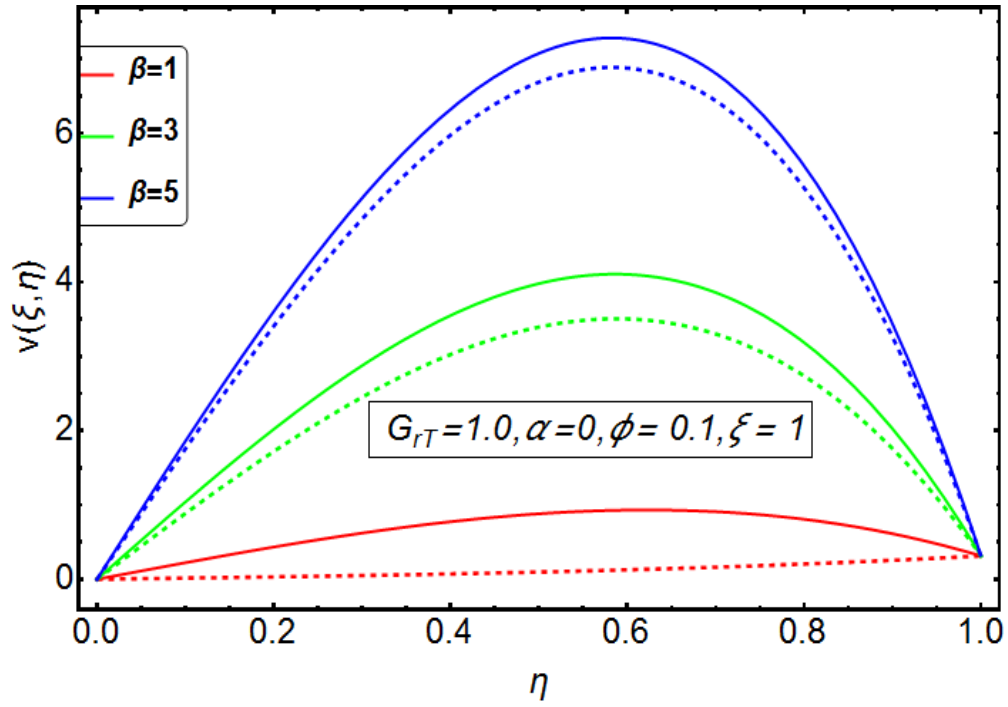


Fig. 3.4(a) Transverse velocity profile ($v(\xi, \eta)$ vs η) for various values of β where $\alpha=0$ (i.e. uniform channel).

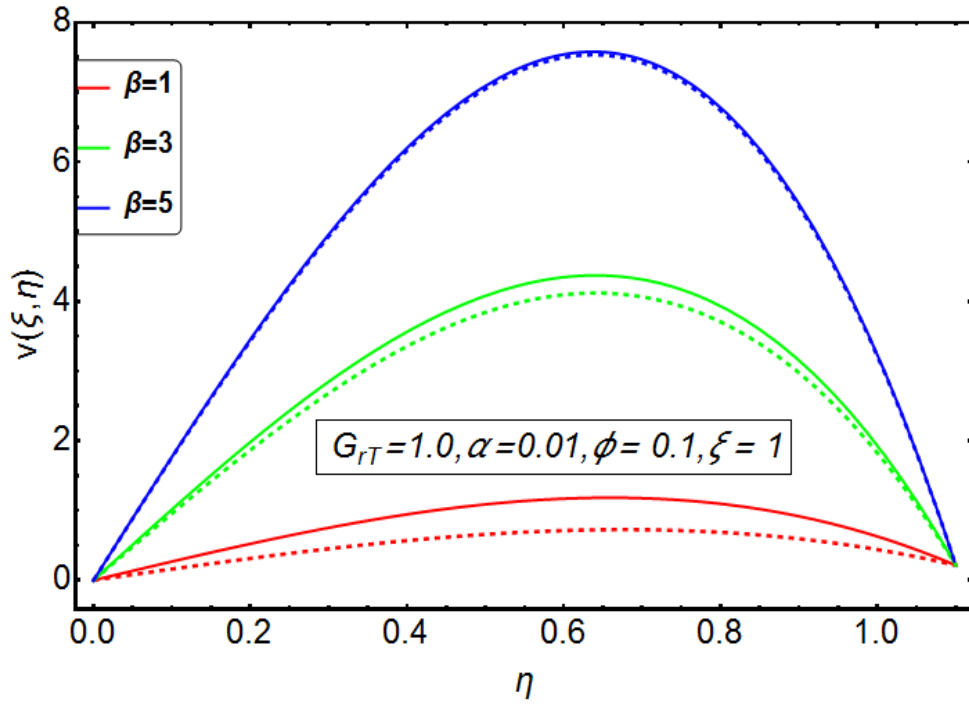


Fig. 3.4(b) Transverse velocity profile ($v(\xi, \eta)$ vs η) for various values of β where $\alpha=0.01$ (i.e. non-uniform channel).

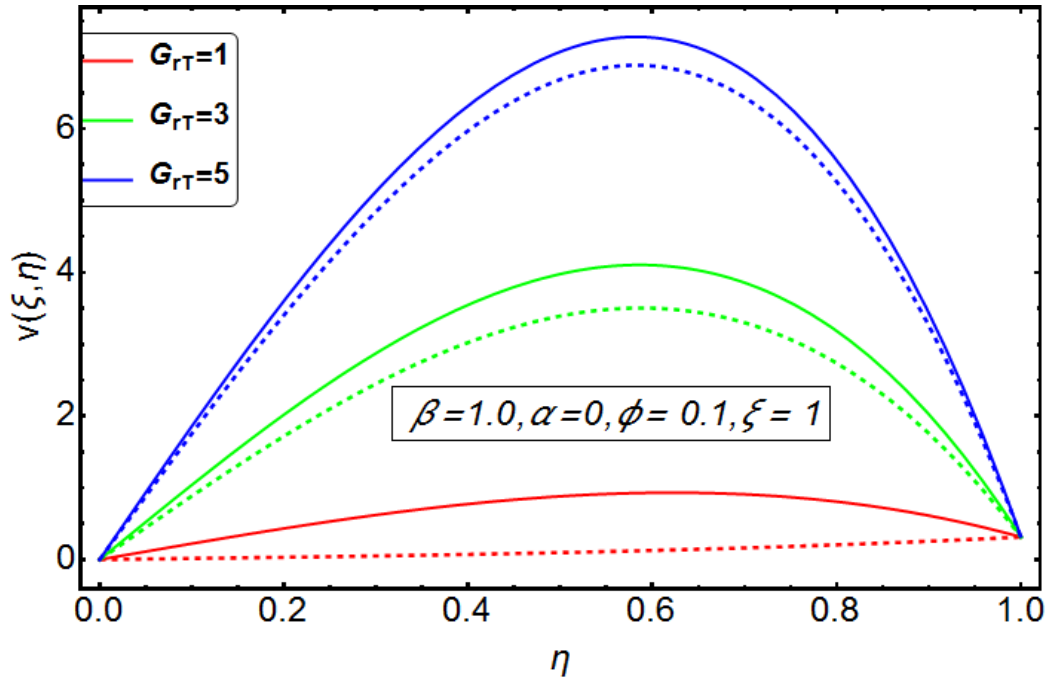


Fig. 3.4(c) Transverse velocity profile ($v(\xi, \eta)$ vs η) for various values of Gr_T where $\alpha = 0$ (i.e. uniform channel).

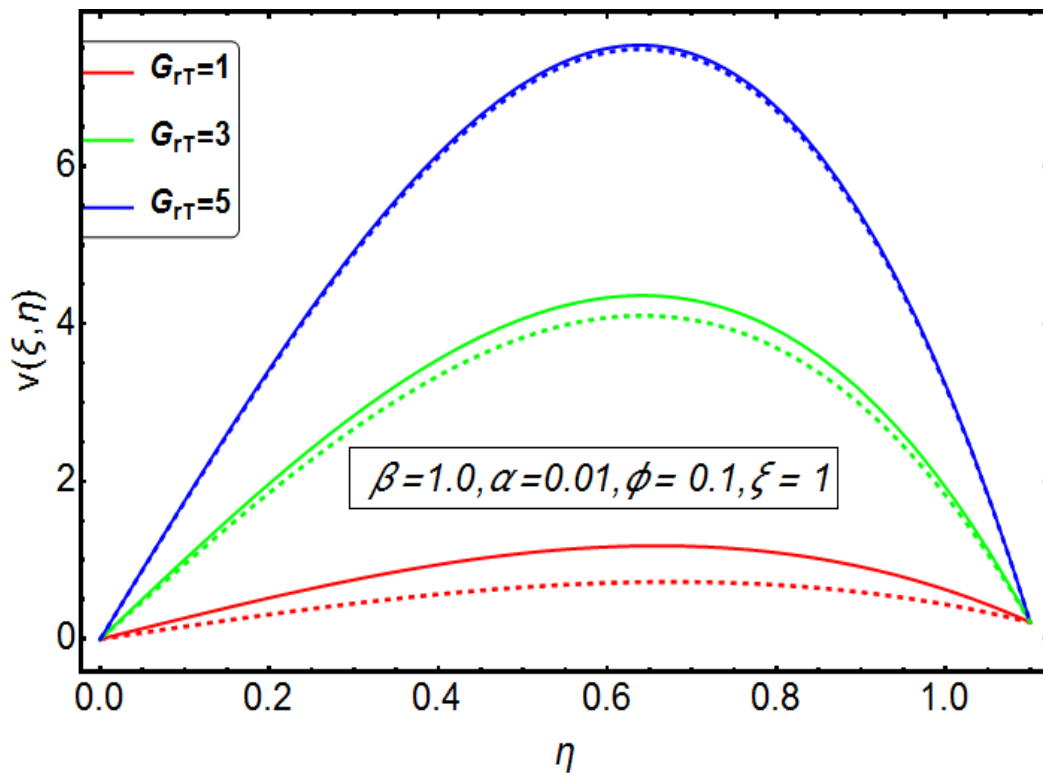


Fig. 3.4(d) Transverse velocity profile ($v(\xi, \eta)$ vs η) for various values of Gr_T where $\alpha = 0.01$ (i.e. non-uniform channel).

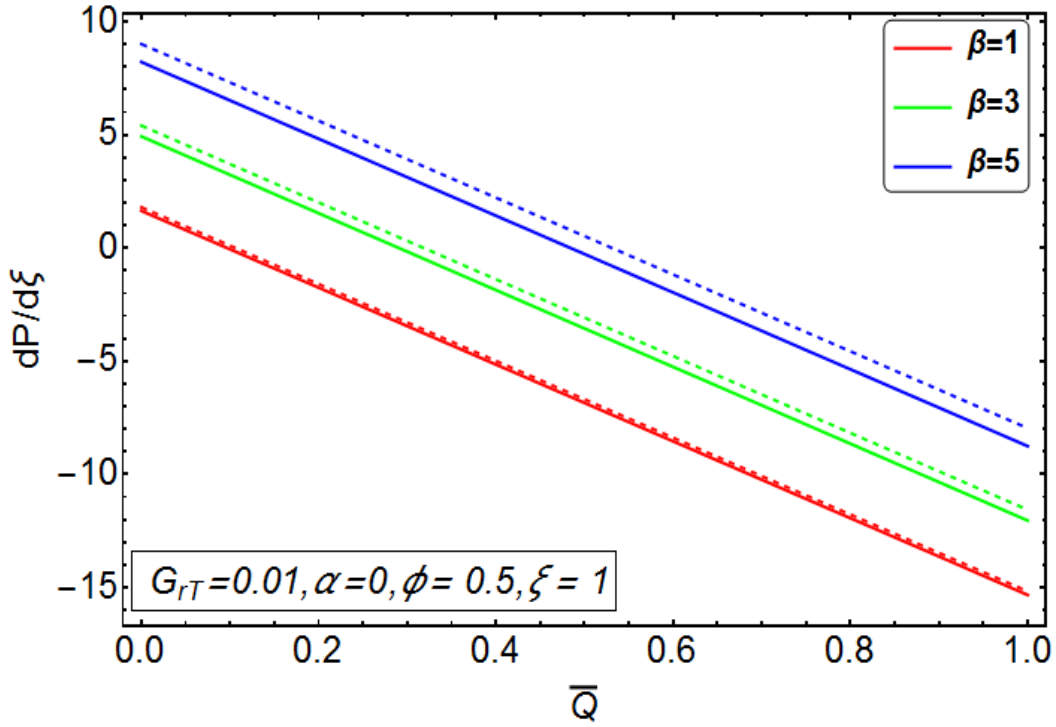


Fig. 3.5(a) Pressure gradient by taking discrete values of β with $\alpha = 0$ (i.e. uniform channel).

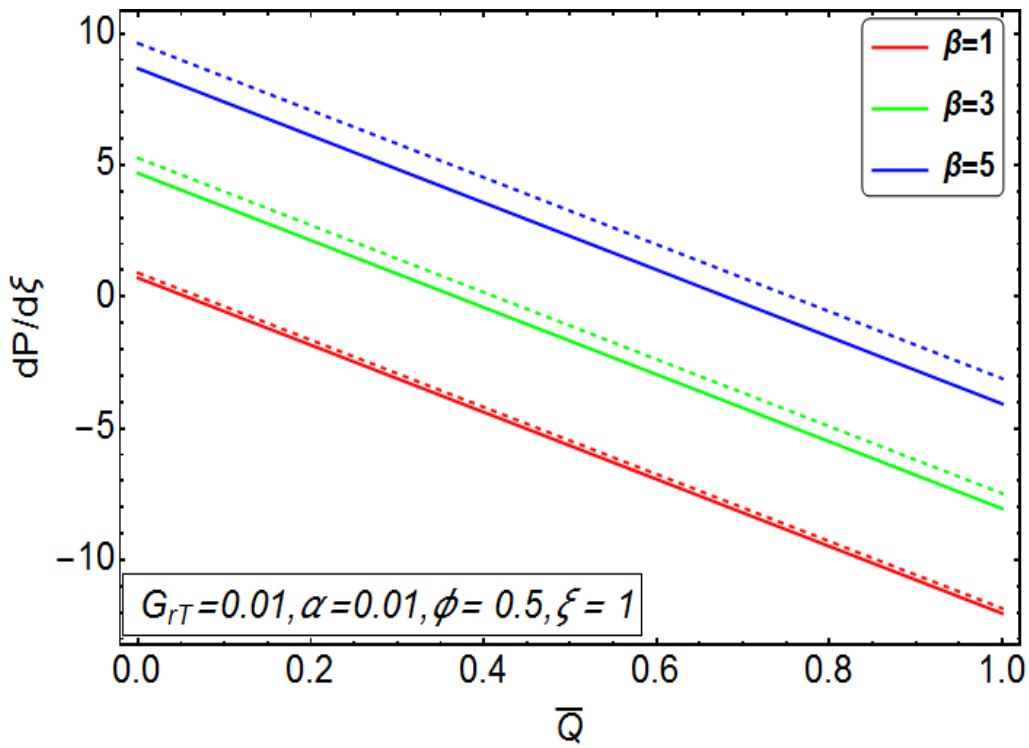


Fig. 3.5(b) Pressure gradient by taking discrete values of β with $\alpha = 0.01$ (i.e. non-uniform channel).

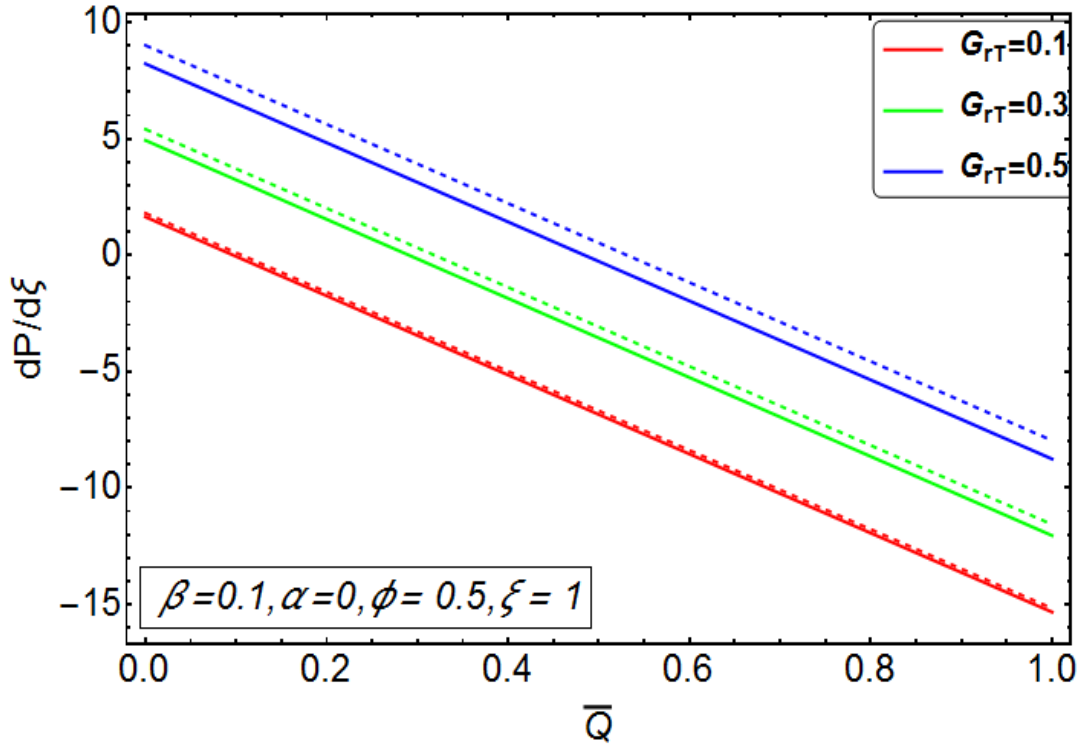


Fig. 3.5(c) Pressure gradient by taking discrete values of Gr_T with $\alpha = 0$ (i.e. uniform channel).

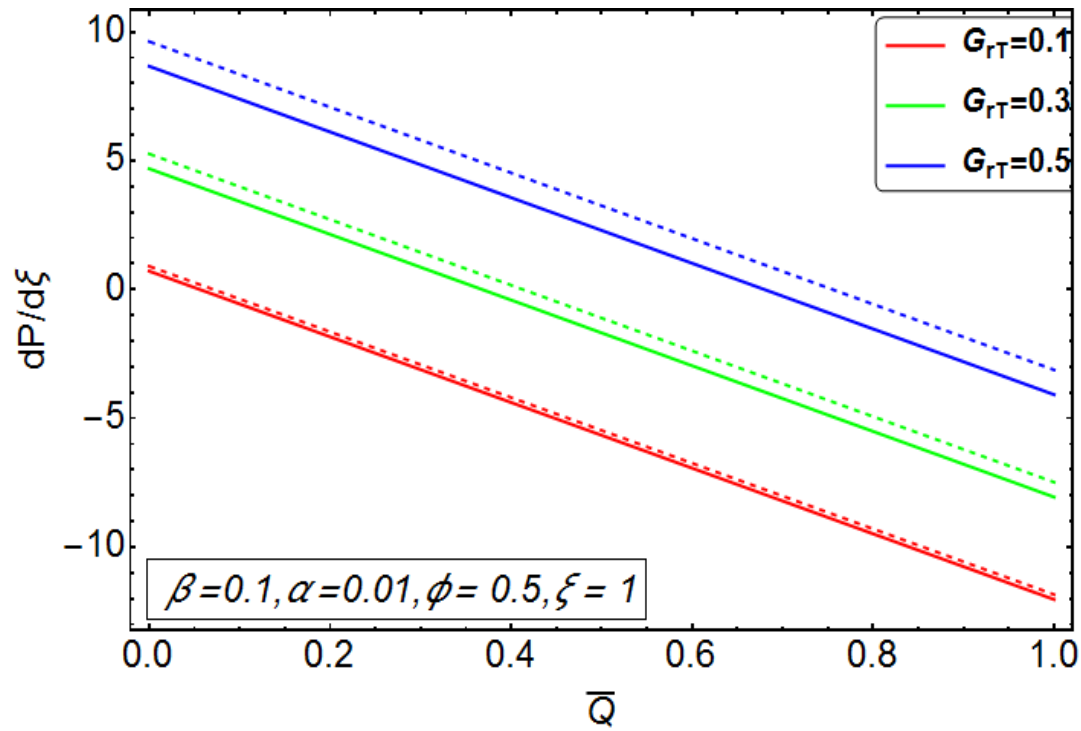


Fig. 3.5(d) Pressure gradient by taking discrete values of Gr_T with $\alpha = 0.01$ (i.e. non-uniform channel).

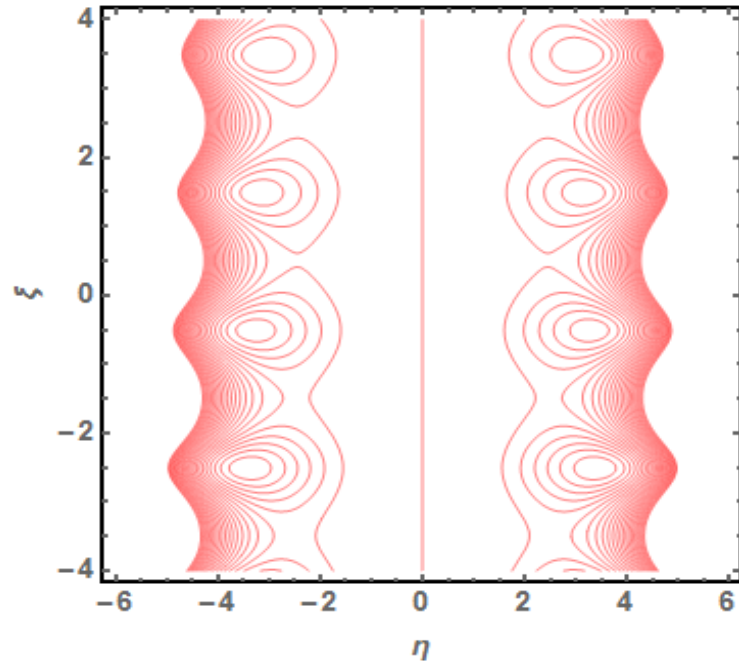


Fig. 3.6(a) Streamlines (SWCnt) for $\beta = 60$ and other parameters are $\epsilon = 0.1$;

$t = 0.5$; $\phi = 0.1$; $\delta = 0.1$; $\alpha = 0.001$; $Gr_T = 0.01$; $\bar{Q} = 50$.

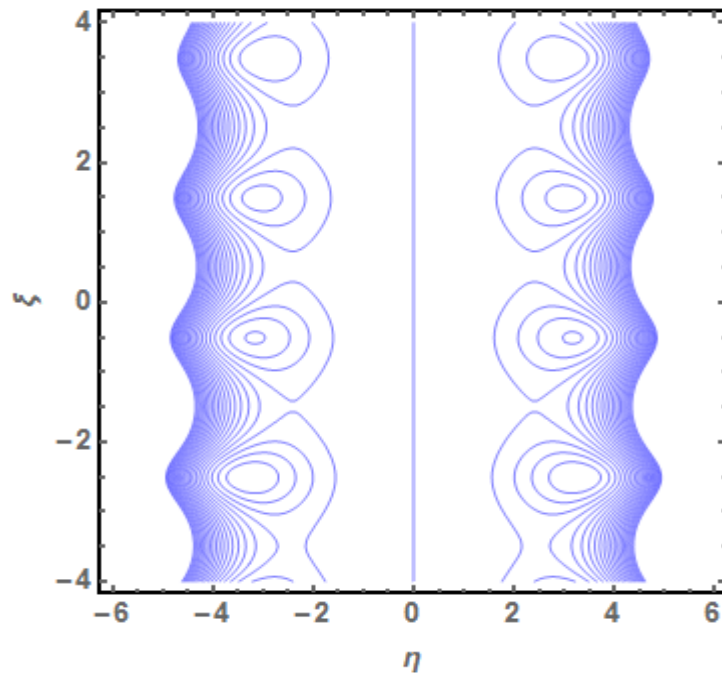


Fig. 3.6(b) Streamlines (SWCnt) for $\beta = 65$ and other parameters are $\epsilon = 0.1$;

$t = 0.5$; $\phi = 0.1$; $\delta = 0.1$; $\alpha = 0.001$; $Gr_T = 0.01$; $\bar{Q} = 50$.

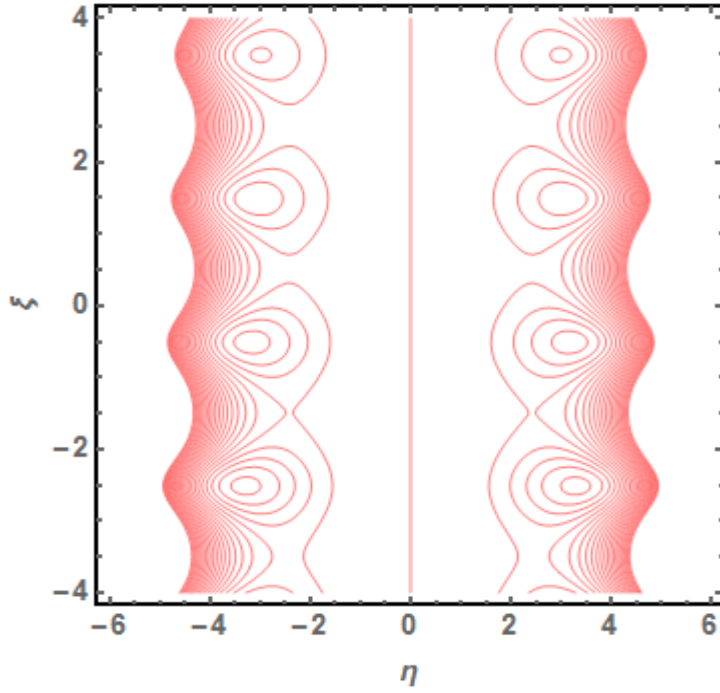


Fig. 3.7(a) Streamlines (MWCnt) for $\beta = 60$ and other parameters are $\epsilon = 0.1$;

$$t = 0.5; \phi = 0.1; \delta = 0.1; \alpha = 0.001; Gr_T = 0.01; \bar{Q} = 50.$$

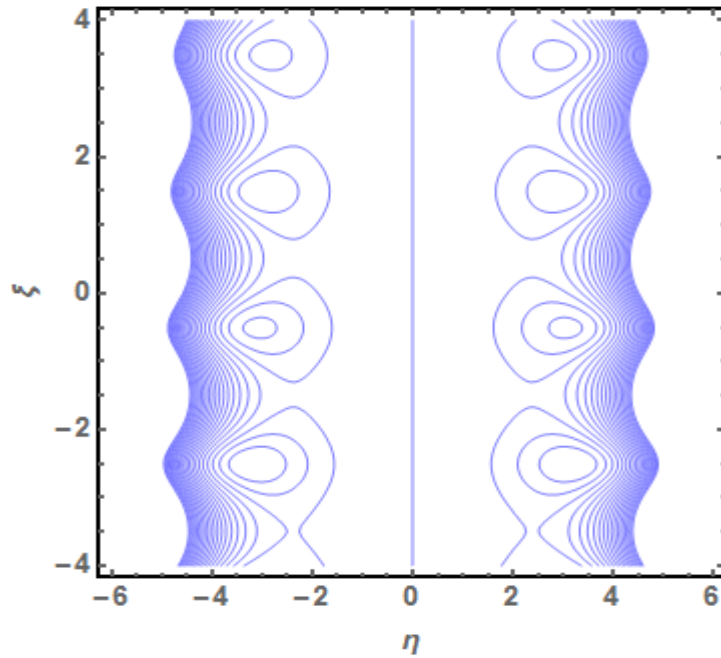


Fig. 3.7(b) Streamlines (MWCnt) for $\beta = 65$ and other parameters are $\epsilon = 0.1$;

$$t = 0.5; \phi = 0.1; \delta = 0.1; \alpha = 0.001; Gr_T = 0.01; \bar{Q} = 50.$$

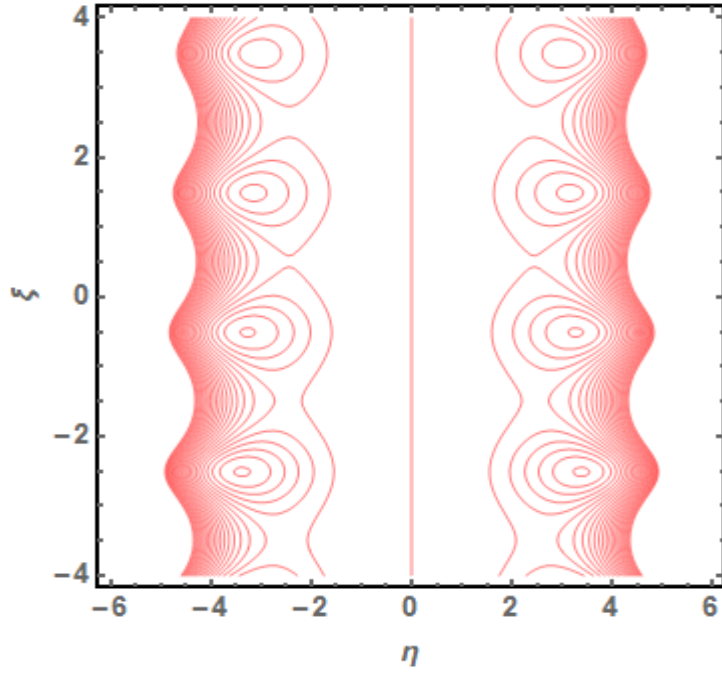
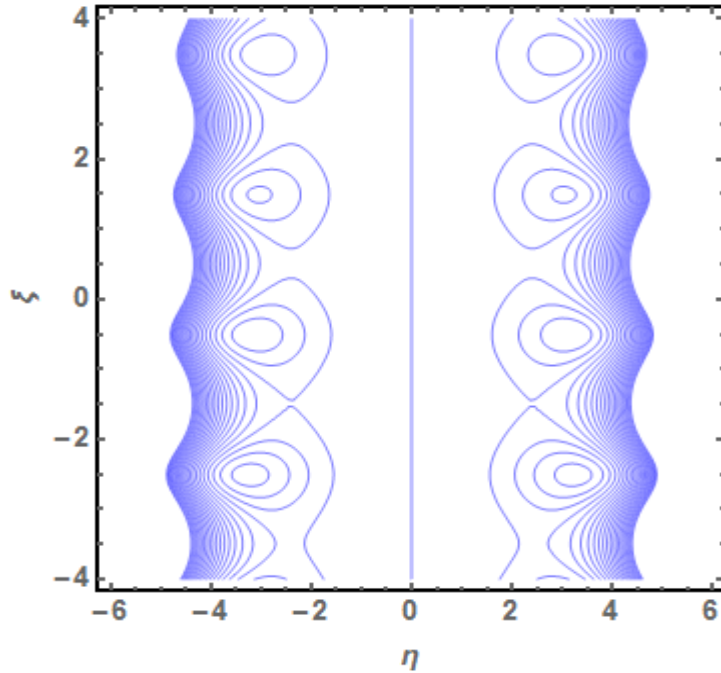


Fig. 3.8(a) Streamlines (SWCnt) for $Gr_T = 60$ and other parameters are $\epsilon = 0.1$;

$$t = 0.5; \phi = 0.1; \delta = 0.1; \alpha = 0.001; \beta = 0.01; \bar{Q} = 50.$$



Figs. 3.8(b) Streamlines (SWCnt) for $Gr_T = 65$ and other parameters are $\epsilon = 0.1$;

$$t = 0.5; \phi = 0.1; \delta = 0.1; \alpha = 0.001; \beta = 0.01; \bar{Q} = 50.$$

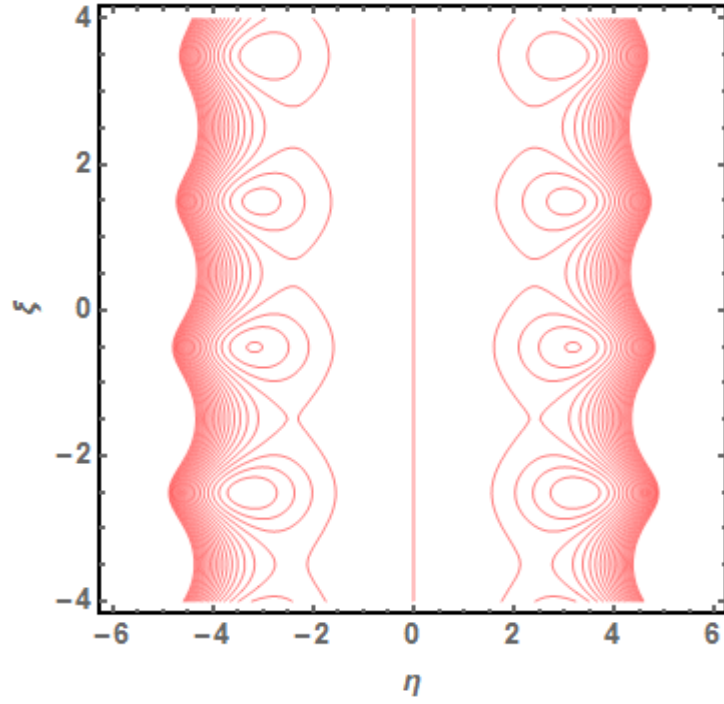


Fig. 3.9(a) Streamlines (MWCnt) for $Gr_T = 60$ and other parameters are $\epsilon = 0.1$;

$$t = 0.5; \phi = 0.1; \delta = 0.1; \alpha = 0.001; \beta = 0.01; \bar{Q} = 50.$$

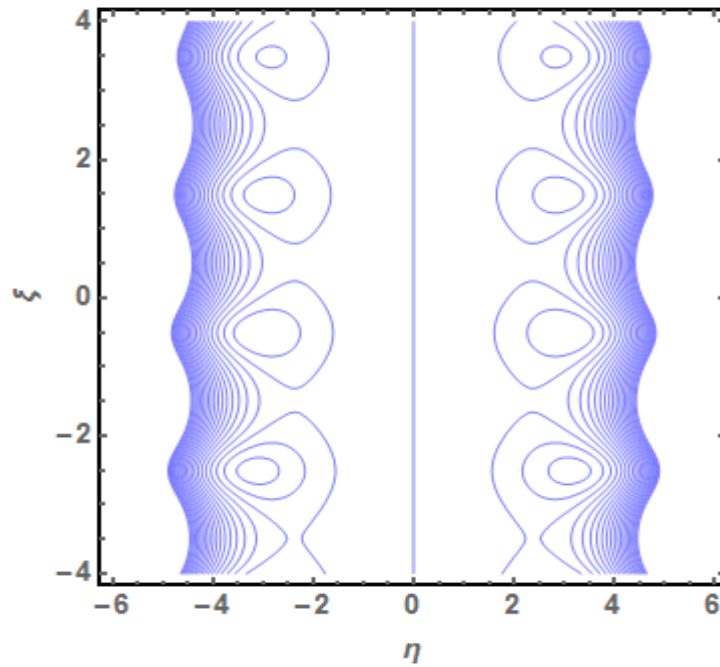


Fig. 3.9(b) Streamlines (MWCnt) for $Gr_T = 65$ and other parameters are $\epsilon = 0.1$;

$$t = 0.5; \phi = 0.1; \delta = 0.1; \alpha = 0.001; \beta = 0.01; \bar{Q} = 50.$$

3.5. Conclusions:

1. Single wall carbon nanotubes attain higher thermal conductivity.
2. In the case of multi wall carbon nanotubes, temperature rise is marginally greater.
3. The axial velocity increases by increasing both β and Gr_T .
4. The axial velocity gains more magnitude for MWCnt than that of SWCnt.
5. The transverse velocity increases by increasing both β and Gr_T .
6. The transverse velocity gains more magnitude for SWCnt than that of MWCnt.
7. The pressure gradient shows linear behaviour and it is directly proportional to both β and Gr_T .
8. Trapped boluses decreases in number by increasing β and Gr_T for both SWCnt and MWCnt.
9. Size of boluses reduces by increasing β and Gr_T for both SWCnt and MWCnt.

References:

1. Pozrikidis C (1987) A study of peristaltic flow. *J Fluid Mech* 180:515-527.
2. Radhakrishnamacharya G (1982) Long wavelength approximation to peristaltic motion of a power law fluid. *Rheol Acta* 21(1):30-35.
3. Wang XQ, Mujumdar AS (2007) Heat transfer characteristics of nanofluids: a review. *Int J Therm Sci* 46(1):1-19.
4. Li M, Brasseur JG (1993) Non-steady peristaltic transport in finite-length tubes. *J Fluid Mech*, 248:129-151.
5. Cremer J, Segota I, Yang CY, Arnoldini M, Sauls JT, Zhang Z, Gutierrez E, Groisman A, Hwa T (2016) Effect of flow and peristaltic mixing on bacterial growth in a gut-like channel. *P Natl Acad Sci USA* 113(41):11414:11419.
6. Bhatti MM, Abbas MA, Rashidi MM (2016) Analytic Study of Drug Delivery in Peristaltically Induced Motion of Non-Newtonian Nanofluid. *J Nanofluids* 5(6):920-927.
7. Bhatti MM, Zeeshan A, Ellahi R (2016) Heat transfer analysis on peristaltically induced motion of particle-fluid suspension with variable viscosity: Clot blood model. *Comput Meth Prog Bio* 137:115-124.
8. Yu W, France DM, Routbort JL, Choi SU (2008) Review and comparison of nanofluid thermal conductivity and heat transfer enhancements. *Heat Transfer Eng* 29(5):432-460.
9. Kakac S, Pramuanjaroenkij A (2009) Review of convective heat transfer enhancement with nanofluids. *Int J Heat Mass Tran* 52(13-14):3187-3196.
10. Akbar NS, Maraj EN, Butt AW (2014) Copper nanoparticles impinging on a curved channel with compliant walls and peristalsis. *Eur Phys J Plus* 129:183.
11. Akbar NS, Butt AW, Noor NFM (2014) Heat Transfer Analysis on Transport of Copper Nanofluids Due to Metachronal Waves of Cilia. *Curr Nanosci* 10(6):807-815.
12. Abdul KR, Kafafy R, Salleh HM, Faris WF (2012) Enhancing the efficiency of polymerase chain reaction using graphene nanoflakes. *Nanotechnology* 23(45): 455106.
13. Akbar NS, Butt AW (2015) Carbon nanotubes analysis for the peristaltic flow in curved channel with heat transfer. *Appl Math Comput* 259:231-241.

14. Akbar NS, Butt AW (2016) Carbon nanotube (CNT) suspended nanofluid analysis due to metachronal beating of cilia with entropy generation. *J Braz Soc Mech Sci & Eng* 2016:1-12.
15. Akbar NS, Nadeem S, Hayat T, Hendi AA (2012) Study of Peristaltic flow of a nanofluid in a non-uniform tube, *Heat mass transfer* 48:451 – 459.
16. Mahian O, Kianifar A, Kalogirou SA, Pop I, Wongwises S (2013) A review of the applications of nanofluids in solar energy. *Int J Heat Mass Tran* 57(2):582-594.
17. Ellahi R, Rahman SU, Nadeem S, Akbar NS (2014) Influence of Heat and Mass Transfer on Micropolar Fluid of Blood Flow Through a Tapered Stenosed Arteries with Permeable Walls. *J Comput Theor Nanosci* 11(4):1156-1163.
18. Bhatti MM, Ellahi R, Zeeshan A (2016) Study of variable magnetic field on the peristaltic flow of Jeffrey fluid in a non-uniform rectangular duct having compliant walls. *J Mol Liq* 222:101-108.
19. Ellahi R, Hassan M, Zeeshan A (2015) Shape effects of nanosize particles in Cu-H₂O nanofluid on entropy generation. *Int J Heat Mass Tran* 81:449-456.
20. Ellahi R, Zeeshan A, Hassan M (2016) Particle shape effects on marangoni convection boundary layer flow of a nanofluid. *Int J Numer Method H* 26(7):2160-2174.
21. Ellahi R, Hassan M, Zeeshan A, Khan AA (2016) Shape effects of nanoparticles suspended in HFE-7100 over wedge with entropy generation and mixed convection. *Appl Nanosci* 6(5):641-651.
22. Ellahi R, Hassan M, Zeeshan A (2015) Study on magnetohydrodynamic nanofluid by means of single and multi-walled carbon nanotubes suspended in a salt water solution, *IEEE Transactions on Nanotechnology*. 14 (4):726 – 734.
23. Zueco J, Prasad VR, Beg OA, Takhar HS (2011) Study of thermophoretic hydromagnetic dissipative heat and mass transfer with lateral mass flux, heat source, ohmic heating and thermal conductivity effects. *29:2808 – 2815*.
24. Kuznetsov AV, Nield DA (2009) Study of Natural convective boundary-layer flow of a nanofluid past a vertical plate. *Int J therm Sci* 49:243 – 247.
25. Fung YC, Yih CS (1968) Study of peristaltic transport. *ASME J Appl Mech* 35: 669 – 675
26. Tripathi D, A mathematical model for swallowing of food bolus through the oesophagus under the influence of heat transfer, *Int. J. Therm. Sci.* 51 (2012) 91–101.

27. Pandey SK, Tripathi D, Influence of magnetic field on the peristaltic flow of a viscous fluid through a finite-length cylindrical tube, *Appl. Bionics Biomech.* 7 (2010) 169–176.
28. Nield DA, Kuznetsov AV, The onset of double-diffusive convection in a nanofluid layer, *Int. J. Heat Fluid Flow* 32 (2011) 771–776.
29. Tripathi D, A mathematical model for the peristaltic flow of chyme movement in small intestine, *Math. Biosci.* 233 (2011) 90–97.
30. Tripathi D, Numerical study on creeping flow of Burgers' fluids through a peristaltic tube, *ASME J. Fluids Eng.* 133 (2011) 121104-1–121104-9.
31. Tripathi D, Numerical study on peristaltic flow of generalized Burgers' fluids in uniform tubes in presence of an endoscope, *Int. J. Numer. Methods Biomed. Eng.* 27 (2011) 1812–1828.
32. Tripathi D, Peristaltic transport of fractional Maxwell fluids in uniform tubes: application of an endoscope, *Comput. Math. Appl.* 62 (2011) 1116– 1126.
33. Tripathi D, Numerical study on peristaltic transport of fractional bio-fluids, *J. Mech. Med. Biol.* 11 (2011) 1045–1058
34. Beg OA, Prasad VR, Vasu B, Reddy NB, Li Q, Bhargava R, Free convection heat and mass transfer from an isothermal sphere to a micropolar regime with Soret/Dufour effects, *Int. J. Heat Mass Transfer* 54 (2011) 9–18.
35. Xue Q. Model for thermal conductivity of carbon nanotube-based composites. *Modern Phys. Lett. B*, 368(2005)302–307.
36. Buongiorno J ,Convective transport in nanofluids,*ASME J.Heat Transfer* 128(2006) 240–250.
37. Nadeem S, Akbar NS,(2008), Effect of heat transfer on the peristaltic transport of MHD Newtonian fluid with variable viscosity: application of Adomian decomposition method *Commun Nonlinear Sci Numer Simul*,3844-3855.
38. Nadeem S, Ijaz S,(2015), Single wall carbon nanotube (SWCNT)examination on blood flow through a multiple stenosed artery with variable nanofluid viscosity, *AIP Adv* 107-217.
39. Nadeem S, Sadaf H,(2016), Hypothetical analysis for peristaltic transport of metallic nanoparticles in an inclined annulus with variable viscosity, *Bull Polish Acad Sci Tech Sci* ,447-454.

40. Huda AB, Akbar NS, Beg OA, Khan MY, (2017), Dynamics of variable-viscosity nanofluid flow with heat transfer in a flexible vertical tube under propagating waves, Results in Physics, 413-425.
41. Tripathi D, Beg OA, A study on peristaltic flow of nanofluids: Application in drug delivery systems, Int J Heat Mass Tran 70(2014)61–70.
42. Akbar NS, Ayub A, Butt AW,(2017),Carbon nanotube analysis for an unsteady physiological flow in a non-uniform channel of finite length,Eur. Phys. J. Plus,132– 177.
43. Akbar NS, Butt AW, Tripathi D,(2017), Nanoparticle Shapes Effects on Unsteady Physiological Transport of Nanofluids through a Finite Length Non-Uniform Channel, Results in Physics.
44. Sheikholeslami M, Ganji DD,(2018) "Biomechanically Driven Nanofluid Flow" , Elsevier BV, 599–614.
45. Akbar NS, Butt AW, Tripathi D,(2017), "Biomechanically driven unsteady non-uniform flow of Copper water and Silver water nanofluids through finite length channel" , Computer Methods and Programs in Biomedicine,1–9.